Estimation of long-term series of total nutrient loads flowing into a large perialpine lake (Lake Como, Northern Italy) from incomplete discrete data by governmental monitoring

Andrea Fenocchi [a,b,*], Fabio Buzzi [c], Claudia Dresti [b], Diego Copetti [d]

[a] *Department of Civil Engineering and Architecture, University of Pavia, Via Ferrata 3, 27100 Pavia, Italy*
[b] *CNR – Water Research Institute, Largo Tonolli 50, 28922 Verbania Pallanza, Italy*
[c] *ARPA Lombardia, Dipartimento di Lecco, Via 1° Maggio 21/B, 23848 Oggiono, LC, Italy*
[d] *CNR – Water Research Institute, Via del Mulino 19, 20861 Brugherio, MB, Italy*

ABSTRACT

Continuous series of nutrient loads released into a water body are essential for nutrient budgeting, water quality modelling and watershed management activities. A quintessential example of pursued data are the series of total nutrient loads flowing from multiple tributaries into a lake. However, except for extraordinary cases in which high-frequency monitoring (HFM) stations are installed for both discharge and concentrations, measured nutrient loads are available on a discrete basis. Such observations are typically obtained by governmental agencies for environmental monitoring purposes, with an at best monthly resolution, yet commonly with gaps spanning years. Usually, monitoring activities are limited to major inflows, neglecting minor ones. However, the latters can play a more relevant role in nutrient load budgets than in hydrological ones, in response to different natural features and pollution among tributary watersheds. In this work, we present a methodology we developed to estimate long-term series of total nutrient loads flowing into a water body, employing as case study Lake Como, a large deep lake in the Italian Alps with manifold monitored and unmonitored tributary watersheds. The method uses observed long-term relationships between discharges and concentrations ($Q – C$) and available discharge measurements and hydrological estimations to estimate continuous load series for the monitored basins. For the unmonitored watersheds, $Q – C$ relationships are estimated from those of the monitored basins, given the observed dependence of the power-law coefficients on basin hydromorphological parameters. This equals to extending the regionalisation approach applied in hydrology for rainfall and discharges to the eco-hydrological field for nutrient load estimation. The application of the method to the case study led to overall annual load estimations congruent to traditional techniques and revealed interesting $Q – C$ watershed dynamics at interannual time scales which could not be disclosed through previous approaches. This work represents an exploratory development and application of ecohydrological regionalisation techniques, whose future development is fostered.

1. Introduction

Lakes whose water quality is of concern are subject to monitoring by governmental institutions, according to principles prescribed by regulations such as the Water Framework Directive 2000/60/EC for the European Union (EU WFD, 2000). Monitoring activities retrieve physical, chemical and biological data for both lakes and their inflows, given the pivotal role of the watershed in determining the lake quality status (Ferreira et al., 2007; Nielsen et al., 2012). Governmental monitoring is generally performed by environmental protection agencies using traditional sampling methods, which produce discrete data of variable time resolution (Bowes et al., 2015; Marcé et al, 2016; Rode et al., 2016). Such resolution varies greatly from one lake to another, and even among seasons for the same lake, passing from fortnightly measurements to gaps of several months according to the relevance of the water body, to the degree of alteration of its natural status and to local regulations (EU

WFD, 2000; Ferreira et al., 2007; Valerio et al., 2022). In many cases, unexpected interruptions in regular data series are present, even spanning years, ascribable to assorted possible inconveniences.

Governmental monitoring of lake waters is ordinarily performed to define their ecological status and verify the suitability for multiple water use (Ferreira et al., 2007; Skeffington et al., 2015; Fu et al., 2020). For lake tributaries, the prevailing aim of governmental monitoring is to keep their quality status under control, ensuring that deterioration of lake water quality is not forthcoming. Only in rare occasions inflow monitoring is aimed at estimating nutrient input loads to the downstream lake (Valerio et al., 2022), even though this would seem the most natural application of such activity. This occurs as the sampling frequency of laboratory measurements, leading to the hereinafter called "measured nutrient loads" (Behrendt, 1996), is usually too loose for a meaningful assessment of input loads. The theoretical estimation of nutrient loads through published land-use-dependent unit export coefficients and wastewater treatment plant (WWTP; a list of symbols and abbreviations is given in Table 1) load percentage reductions, leading to the hereinafter called "estimated nutrient emissions" (Behrendt, 1996), is hence often the only viable approach. This method, which is independent from experimental discharge and concentration measurements,

Table 1
List of symbols and abbreviations.

Abbreviation	Meaning
α	coefficient defining the relevance of R_a over R_u in the definition of $a*$ and $b*$
a	multiplying coefficient of the $Q - C$ power law
A	tributary watershed area
$a*$	transformed a coefficient of the $Q - C$ power law
b	exponent coefficient of the $Q - C$ power law
$b*$	transformed b coefficient of the $Q - C$ power law
C	concentration
c	multiplying coefficient of the $R_u - a*$ power law
CLC	Corine Land Cover
$Cond$	water conductivity at standard 20 °C conditions
CV	coefficient of variation
d	exponent coefficient of the $R_u - a*$ power law
DTM	Digital Terrain Model
e	constant-term coefficient of the $R_u - a*$ power law
f	multiplying coefficient of the $S_m - b*$ power law
g	exponent coefficient of the $S_m - b*$ power law
GIS	Geographic Information System
h	constant-term coefficient of the $S_m - b*$ power law
HFM	high-frequency monitoring
I_a	annual mean liquid inflow of a tributary watershed over a single year
L	length dimension
LLS	linear least squares
LOD	limit of detection
M	mass dimension
max/min	maximum/minimum ratio
NLS	non-linear least squares
$N\text{-}NH_4$	ammonium
$N\text{-}NO_3$	nitrate
p	p-value
$P\text{-}PO_4$	orthophosphate
Q	water discharge
$Q*$	generic index discharge
Q_a	annual mean discharge of a tributary watershed over a single year
$Q_{a,tot}$	annual mean discharge of the whole Lake Como watershed over a single year
Q_m	mean 2000–2019 discharge of a tributary watershed
$Q_{m,tot}$	mean 2000–2019 discharge of the whole Lake Como watershed
r	Pearson regression coefficient
R_a	agricultural ratio of a tributary watershed
R_u	urban ratio of a tributary watershed
SD	standard deviation
S_m	mean slope of a tributary watershed
T	time dimension
TN	total nitrogen
TP	total phosphorus
WWTP	wastewater treatment plant

results however in single nutrient emission values for a watershed (Rast and Lee, 1983). These are unconnected to the hydrological variability and descend from the employed load indices from literature, which hardly consider the specific features of the basin (Behrendt, 1996; Yang et al., 2019). Furthermore, large mountain lakes, such as the European perialpine ones (Dresti et al., 2021), typically have a multitude of inflows coming from multiple side valleys (Fenocchi et al., 2019). Usually, only the most relevant tributaries, defined according to water quantity and/or quality criteria, are monitored, precluding the estimation of total loads. Diffuse loads, whose monitoring is largely unviable, also play a relevant role for many lakes (Janssen et al., 2019).

Because of these limitations, data on tributaries available from governmental agencies are generally not apt for the direct use in coupled lake hydrodynamic-ecological numerical models, for which continuous series of total input loads at typically daily resolution are needed (Fenocchi et al., 2019; Dresti et al., 2021). Such total continuous series are usually generated from available discrete data, filling temporal gaps for monitored tributaries by linear interpolation and computing the load series for the unmonitored ones assuming values proportional to gauged inflows according to the watershed area (Tartari et al., 2006). These practices can lead to relevant inaccuracies, as: (1) short-term hydrological events such as floods, playing a relevant role in nutrient delivery (Viviano et al., 2017; Salerno et al., 2018; Copetti et al., 2019), may be missed in the performed interpolations; (2) small yet highly anthropised unmonitored basins can bring to the lake nutrient loads per unit area which are far larger than the mean values obtained for the monitored tributaries.

To reduce the shortcomings in the generation of continuous load series from discrete monitoring data, the $Q - C$ relationships between discharges (Q) and nutrient concentrations (C) should be first obtained for each basin, calibrating them from available data. This way, nutrient load estimations could be reduced to discharge estimations. For monitored tributaries, discharge measurements are usually much more frequent than biochemical samples (Cartwright, 2020), considering that automatic stations are typically installed for flood hazard and water balance issues. For ungauged tributaries, discharges can be estimated from hydrological estimation techniques. To obtain the related concentrations, the $Q - C$ relationships found for the monitored basins could be extrapolated to the neighbouring unmonitored ones according to proper laws, based on relevant watershed properties such as land use and morphometry. This would translate into expanding to the ecohydrological field the regionalisation approach commonly applied in hydrology (He et al., 2011; Guo et al., 2021) to estimate rainfalls and discharges at unmonitored points, basing on the data measured in neighbouring monitored stations. This is something which to the knowledge of the Authors has never been organically attempted before.

Using these tools, it would be possible to obtain for lakes subject to ordinary governmental monitoring continuous total nutrient load estimations which consider the hydrological variability as well as the peculiar $Q - C$ relationships of each tributary basin, including unmonitored ones. These estimated series, in addition to modelling activities, could support the management of the tributaries themselves, of their watersheds, and of the downstream lake, including algal bloom issues (Moatar et al., 2017; Cartwright, 2020). As a matter of fact, these instruments could be applied not only to lake watersheds, but in all situations in which obtaining continuous load series from discrete monitoring data on rivers and extending them to neighbouring unmonitored basins is desired. Furthermore, availability of robust $Q - C$ relationships could limit the need for high-frequency monitoring (HFM) stations for biochemical variables (Bowes et al., 2015; Marcé et al, 2016; Rode et al., 2016; Tiberti et al. 2021) to streams of specific environmental concern (D'Amario et al., 2021).

In this study, we present an exploratory attempt at developing such an approach for total continuous input load estimation, including ecohydrological regionalisation principles. Application is presented to the long-term 2000–2019 series of total nutrient loads flowing into Lake

Como (Northern Italy). Estimations were developed from the monitoring data available from the local regional environmental protection agency ARPA Lombardia. The designed approach proved successful for the case study, paving the way to future research on its improvement and on the assessment of the applicability limits.

2. Materials and methods

2.1. General aspects of Q – C relationships in streams

The dilution behaviour, i.e. the inverse proportionality between Q and C, has been verified to hold under most conditions for dissolved chemical substances such as nutrients and major ions (Shanley et al., 2011; Thomas et al., 2016; Moatar et al., 2017). The dilution chemo-dynamic (i.e., C varies with Q) behaviour thus represents the null hypothesis for such substances (Torres and Baronas, 2021) and is ascribed to the dominance of source-limitation dynamics on solute transport. The opposite concentration behaviour, i.e. the direct proportionality between Q and C, is linked to transport-limited dynamics and is instead typical of suspended sediment transport (Syvitski et al., 2000; Godsey et al., 2019). Nevertheless, the concentration behaviour has been often observed for dissolved substances as well (Thomas et al., 2016; Moatar et al., 2017; Cartwright, 2020). For both dilution and concentration Q – C dynamics, there is a general agreement on the power law as the simplest fit of data (Syvitski et al., 2000; Godsey et al., 2009), even if more complicated fitting approaches have been proposed (Moatar et al., 2017; Botter et al., 2019). The basic formulation of the Q – C power law is:

$$C = aQ^b \tag{1}$$

where the a and b coefficients depend on the considered watershed, substance and time window. For dissolved nutrients, which naturally derive from soil weathering, $-1 < b < 0$ exponents have been mostly attained, with negative values close to 0 being the most common situation. Such values imply a chemodynamic behaviour which tends towards chemostasis (i.e., C is invariant with Q) (Godsey et al., 2009; Musolff et al., 2015; Botter et al., 2019; Godsey et al., 2019; Cartwright, 2020), corresponding to the common observations in which Q varies by more orders of magnitudes than C (Godsey et al., 2009; Moatar et al., 2017). This way, loads are largely proportional to discharges (Moatar et al., 2017), hence highest values are connected to flood events (Maher and Chamberlain, 2014; Torres and Baronas, 2021).

Despite this general theory emerged from decades of research, many open questions remain on the Q – C relationships of dissolved substances (Moatar and Meybeck, 2005; Godsey et al., 2009; Thompson et al., 2011; Bieroza and Heathwaite, 2015; Moatar et al., 2017) and on the role of the basin and of the specific substance in determining the concentrations observed in each case (Basu et al., 2011; Herndon et al., 2015; Torres et al., 2015; Moatar et al., 2017). In fact, the same substance may behave differently across basins (Godsey et al., 2009; Moon et al., 2014; Torres et al., 2015, 2017) and, over the same basin, according to the considered time window (Herndon et al., 2015; Torres et al., 2015; Botter et al., 2019). Land use strongly shapes nutrient concentrations (Musolff et al., 2015; Moatar et al., 2017; Abbott et al., 2018; Bieroza et al., 2018; Botter et al., 2019), with a direct dependence on the anthropisation degree (D'Amario et al., 2021), although a high variability of the Q – C behaviour according to basin peculiarities has been reported (Godsey et al., 2019). It has been proven that dilution laws are more precisely followed by conservative substances, and much more uncertainty by non-conservative ones such as nutrients, due to the intervention of biochemical factors, emerging under low-flow discharges (Bowes et al., 2015; Duncan et al., 2017; Moatar et al., 2017; Balerna et al., 2021).

A hysteretic behaviour with different Q – C trends between the ascending and descending limbs of flood hydrographs has been often observed in anthropised basins when HFM measurements have been performed, in turn different from the general dilution behaviour observable from long-term low-frequency measurements over the same site (House and Warwick, 1998; Godsey et al., 2009; Duncan et al., 2017; Moatar et al., 2017; Minaudo et al., 2019; Knapp et al., 2020; D'Amario et al., 2021). These short-term dynamics are due to phenomena such as the dissolution of nutrients stored within the soil for agricultural watersheds or within sewer sediments for urban ones (Bowes et al., 2015; Moatar et al., 2017; Knapp et al., 2020). Another relevant source of short-term Q – C anomalies in urban basins is the activation of Combined-Sewer Overflows (CSOs), leading to the release of untreated sewage in water bodies, enriched by the washout of polluted impervious areas (Arthur and Ashley, 1998; Viviano et al., 2014; Copetti et al., 2019). These phenomena may lead to short-term concentration dynamics, which nevertheless disappear for the most intense events, in which exceptional discharges bring about the return of source-limited dilution dynamics (Viviano et al., 2017). These complex phenomena make short-term Q – C trends impossible to be parameterised, as each flood exhibits a different behaviour according to the event hydrology and to the pre-existing conditions of the watershed (Bowes et al., 2015; Rode et al., 2016; Knapp et al., 2020). Furthermore, short-term dynamics cannot be grasped by ordinary discrete monitoring, which is though apt at characterising the long-term Q – C behaviour (Godsey et al., 2009; Knapp et al., 2020). When discrete monitoring intercepts these peculiar events, outliers to the long-term trend are produced, which were in the past attributed to measurement errors (Bowes et al., 2015).

2.2. Methodology to estimate Q – C relationships for monitored and unmonitored watersheds

The developed methodology allows estimating the Q – C relationships of dissolved substances in unmonitored basins from those obtained for the neighbouring monitored ones, assuming that ecohydrological similarity factors subsist among watersheds, such as climate and soil characteristics, these being some of the factors which have been proven to determine the variability of the relationships across sites (Moon et al., 2014; Ibarra et al., 2016; Torres et al., 2017).

To obtain Q – C relationships for the monitored basins which could hold for prognostic use, the a and b coefficients of the power law in Eq. (1) were here estimated from monitoring data through non-linear least squares (NLS) using MATLAB®. This was done despite the ordinary linear least squares (LLS) having been traditionally used in studies on Q – C relationships, in which b coefficients are estimated only for comparison among different substances and watersheds. In fact, the flaw of LLS in determining the b coefficients of power laws, due to the linear fit being obtained in the log–log space, is long known in literature (Miller, 1984; Pattyn and Van Huele, 1998; Goldstein et al., 2004; Clauset et al., 2009; Dralle et al., 2015). For $b < 0$ values, such flaw would cause residuals to the power law determined through LLS to diverge exponentially for decreasing Q values, leading to a corresponding underestimation of C and hence of predicted loads. Such problem is avoided through NLS, in which the regression is performed on the variables in their original domain.

Work was then done on the a and b coefficients of Eq. (1) obtained for the monitored basins to make them dependent on some relevant watershed ecohydrological parameters, to allow their extrapolation to unmonitored basins.

The a coefficient was transformed into a comparison metric reflecting basin characteristics by turning it into non-dimensional. As a matter of fact, while b is natively non-dimensional and as such has been widely considered as a comparison metric of the Q – C behaviour across watersheds (Godsey et al., 2009; Torres et al., 2015; Moatar et al., 2017; Botter et al., 2019; Cartwright, 2020), a has the units of C/Q^b, i.e. $\left[MT^b/L^{3(1+b)} \right]$, where M is mass, T is time and L is length. Being correlated to both Q and b, a cannot be directly compared across basins

(Asselman, 2000; Syvitski et al., 2000; Mather and Johnson, 2014; Dralle et al., 2015; Knapp et al., 2020; Torres and Baronas, 2021). In fact, its theoretical meaning of concentration attained for a unit discharge has no practical meaning, as a discharge of 1 m^3/s can be a high, ordinary or insignificant value, depending on the watershed. Decorrelation of a can be performed normalising the discharge in Eq. (1) by a Q^* index value (Mather and Johnson 2014):

$$\frac{C}{(Q^*)^b} = a\left(\frac{Q}{Q^*}\right)^b \rightarrow C = a^*\left(\frac{Q}{Q^*}\right)^b \tag{2}$$

in which the decorrelated a^* coefficient is thus:

$$a^* = a(Q^*)^b \tag{3}$$

Eqs. (2) and (3) allow removing the correlation of a from Q, whatever is the designated Q^*. Complete decorrelation from b instead requires a proper Q^*, as can be obtained from the methodology by Bergner and Zouhar (2000). However, that approach cannot be employed in the present case, as Q^* is estimated by Bergner and Zouhar (2000) as function of the original a and b coefficients of the $Q - C$ regression of the observed values. These are clearly not available for unmonitored basins, which we are addressing in this work. We then used as Q^* the mean watershed discharge Q_m, available for unmonitored basins from hydrological estimations. Such normalisation of Q through Q_m nevertheless removes a large part of the correlation of a from b (Knapp et al., 2020).

The a coefficients of the $Q - C$ regressions estimated for the monitored basins in the case study were found to be positively correlated to the urban ratio R_u of the watersheds. A significant reduction of dispersion was found passing from a to a^*, as detailed in the Results and Discussion section. The obtained correlation is explained by a and especially a^* revealing the magnitude of observed concentrations (Godsey et al., 2019), which largely depends on the degree of anthropisation. The a^* coefficients obtained for the monitored basins could be suitably fitted by the following power law:

$$a^* = c(R_u)^d + e \tag{4}$$

where c, d, e are coefficients, depending on the considered substance. The e coefficient physically represents the a^* for a basin with $R_u = 0$, being that $d > 0$ was always obtained. Fitting was performed through NLS, given the prognostic use of the obtained power law to find the a^* coefficients of the unmonitored basins.

For the b coefficient, Torres et al. (2015) found, comparing the $Q - C$ relationships for neighbouring basins, that stronger dilutions, i.e. negative coefficients farther from zero, were obtained in flatter basins, whereas more sloping basins were more chemostatic. This defined a positive correlation of b with the mean slope S_m, to be ascribed mostly to the high soil erosion ratio of mountain watersheds, in which source-limitation dynamics are hence replaced by transport-limited ones. In our case study, this correlation was partially concealed by basin urbanisation, almost absent in the study area of Torres et al. (2015). In fact, the short-term rainfall dynamics previously described for urban areas surely distort the long-term b coefficients towards values closer to zero. To sort this issue in the simplest possible way, we introduced a corrected b^* coefficient:

$$b^* = bR_u \tag{5}$$

This way, if the b coefficient is drawn nearer to zero by high urbanisation, it is compensated by the high R_u value of the watershed itself. Through the correction, we were able to significantly reduce dispersion in the regressions with S_m, as detailed in the Results and Discussion section. The b^* coefficients obtained for the monitored basins were suitably fitted by another power law:

$$b^* = f(S_m)^g + h \tag{6}$$

where f, g, h are coefficients, depending on the considered substance. As $g < -1$ was always found, h defines the asymptotical value reached by

b^* for high slopes. Fitting was again performed through NLS.

Through the regressions developed for monitored basins through Eqs. (4) and (6), the a^* and b^* transformed coefficients can be computed for unmonitored basins. The original b and a coefficients can be computed from them reversing in sequence Eqs. (5) and (3), respectively, finally allowing the estimation of concentrations through measured or hydrologically estimated discharges in unmonitored basins through Eq. (1). Three watershed hydromorphological parameters are then needed for the application of the elaborated method:

1) the mean discharge Q_m, which contributes to the a coefficient;
2) the mean slope S_m, which contributes to the b coefficient;
3) the urban ratio R_u, which contributes to both the a and b coefficients.

2.3. Case study

Lake Como (Fig. 1) is a deep perialpine lake at the foothills of the Central Italian Alps. It has a remarkable environmental and economic value, its waters being used for drinking supply by the cities of Como and Lecco (Fig. 1b) and by other towns, fishery and highly profitable recreational activities, in addition to large-scale agricultural and industrial use of the outflowing water (Copetti et al., 2020). Lake Como is the deepest Italian lake, with a 426 m maximum depth and a 181 m mean depth according to the standard lake surface elevation of 198 m a.s.l. (Rogora et al., 2018) and the 2005 bathymetry by the Italian Navy (Regione Lombardia, *unpublished data*). The corresponding surface area and volume are respectively 145.4 km^2 and 26.0 km^3, making it the third Italian lake for both properties. The total watershed area including the lake estimated through our GIS analysis (Fig. 1a) is 4547.5 km^2, 89.4% of which lies in Italy and 10.6% in Switzerland. The watershed has a maximum elevation of 4020 m a.s.l. at Piz Bernina and an average elevation of 1558 m a.s.l. Lake Como, which covers only 3.2% of its watershed, has a peculiar Y-like shape (Guyennon et al. 2014; Copetti et al. 2020), with three narrow elongated arms. It has two main tributaries, inflowing River Adda and River Mera (Fig. 1a), which enter at the northern edge of the lake and drain the large Valtellina and Valchiavenna valleys, respectively, which include mountain regions of perpetual snow (Fig. 1b). The two rivers had a mean discharge in the 2000–2019 study period according to present estimations of 90.3 m^3/s and 33.5 m^3/s, respectively. The Adda basin covers 57.5% of the total watershed, while the Mera basin 16.3% of it. There are also 17 minor tributaries with a discernible watershed (Fig. 1a), covering altogether 16.9% of the total basin. The remnant 6.1% of the watershed is covered by strips surrounding the lake made up of very small, hardly distinguishable watersheds which drain into the lake as diffuse sources or through ephemeral creeks (Fig. 1a). The only emissary of Lake Como is outflowing River Adda, whose mean discharge at the Olginate regulation dam (Fig. 1a) was equal to $Q_m = 160.0$ m^3/s in the 2000–2019 study period (ARPA Lombardia, 2022). Mean annual liquid inflows (summation of rainfall and snowmelt) over the Lake Como watershed for 2000–2019 from the present hydrological estimations were 1268 mm. A significant variability was observed between dry and wet years, with a 777 mm minimum in 2005 and a 1721 mm maximum in 2014. The northern Adda and Mera basins are the driest ones, with 1117 mm and 1398 mm mean annual liquid inflows, respectively. The remnant part of the watershed has similar mean annual values, ranging between 1458 mm for the Cosia basin and 1689 mm for the Albano basin (Fig. 1a).

Lake Como, as the other Italian perialpine lakes, underwent eutrophication in the 1960s, reaching peak eutrophic conditions in the early 1980s (Salmaso and Mosello, 2010). Restoration measures triggered a slow reversal towards mesotrophic conditions, which stabilised by the mid-2000s (Rogora et al., 2018). This was mostly allowed by the connection of sewers of lake-facing towns to WWTPs. Pollution is prominent in the closed south-western arm, which does not have an emissary, is partially separated from the rest of the lake by an underwater ridge and receives the waters of the heavily polluted Creek Cosia
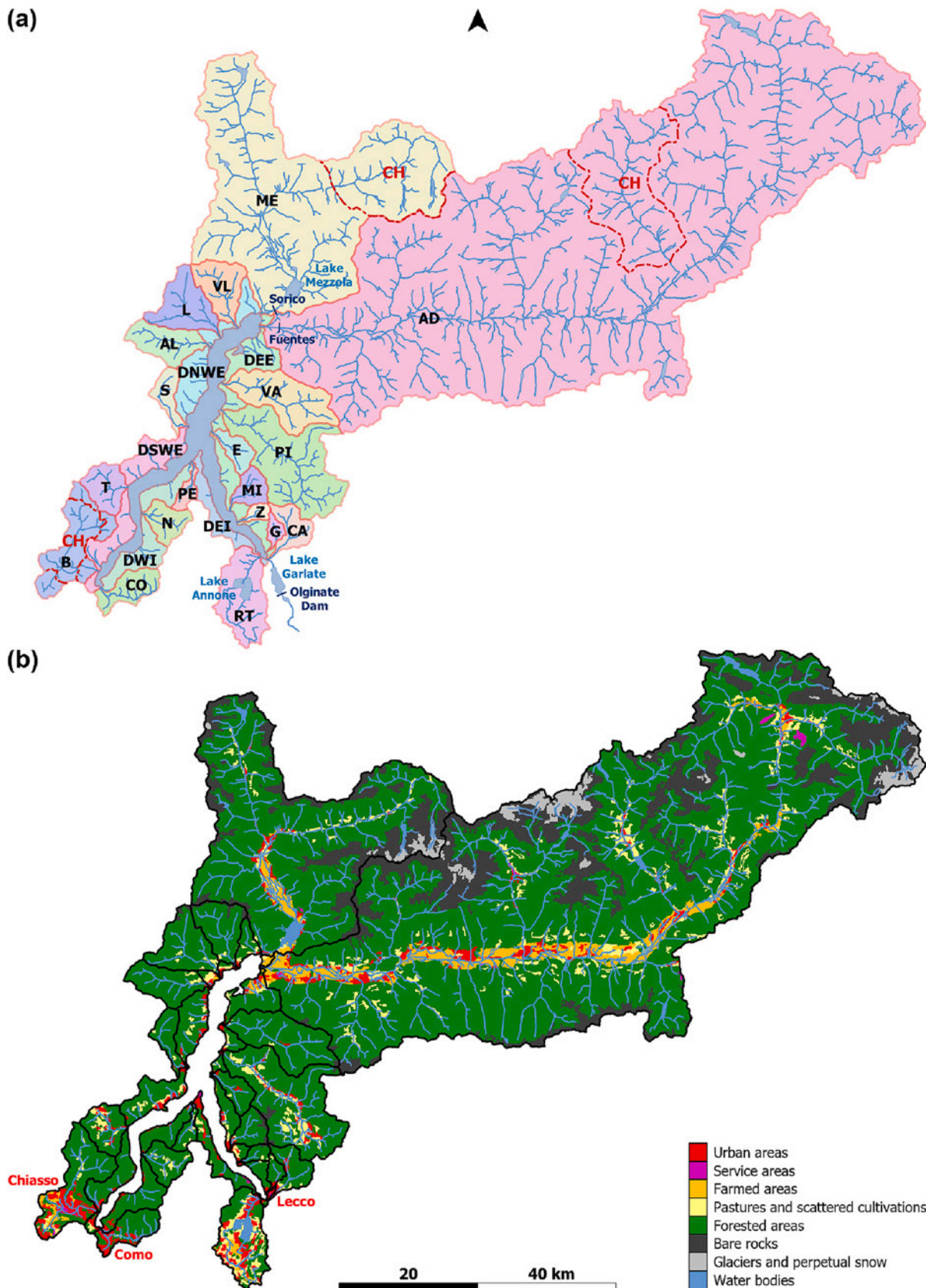
Fig. 1. (a) Tributary basins of Lake Como from the GIS analysis and relevant hydrographic elements (basin abbreviations are given in Table 2; CH = Swiss territory); (b) map of land use groups for the Lake Como watershed from the CLC 2018 data, indicating the main urban areas.

(1.5 m^3/s 2000–2019 mean discharge) and Creek Breggia (4.0 m^3/s 2000–2019 mean discharge), which drain the Como and Chiasso urban areas (Fig. 1b), respectively (Bettinetti et al., 2000; Copetti et al., 2020). Another peculiar tributary is Creek Rio Torto (3.5 m^3/s 2000–2019 mean discharge) in the south-eastern arm, which drains a heavily urbanised basin, a significant part of which is yet placed upstream of Lake Annone (Fig. 1a), a twin-basin lake with total 5.5 km^2 surface area, 30.8 hm^3 volume and 11 m maximum depth (Osservatorio dei Laghi Lombardi, 2005), of which Creek Rio Torto is the only emissary.

The sole existing proper estimations of total nutrient loads flowing into Lake Como were produced inside the PLINIUS project for the restoration of Lake Como (Gruppo di Lavoro Lago di Como, 2006). The regional governmental authority Regione Lombardia considers those estimations as reference for current environmental management activities. Both estimated nutrient emissions and measured nutrient loads over the whole Lake Como watershed were assessed within the PLINIUS project. For the formers, a 274 t a^{-1} value was determined for total phosphorus (*TP*) (Salerno and Buraschi, 2006). For the latters, mean annual values of 265 t a^{-1} for *TP* and 7871 t a^{-1} for total nitrogen (*TN*) were established over the 2000–2004 period (Tartari et al., 2006). The evaluation of measured nutrient loads assumed for the monitored basins the mean 2000–2004 observed concentrations and discharges obtained as follows: 1) through measurements for River Adda; 2) through regressions from the formers for River Mera; 3) through a subdivision of the remnant part of the annual hydrological balance according to area and long-term mean precipitation for the other monitored tributaries. For all unmonitored watersheds, a fixed identical concentration was employed, calculated averaging the mean observed concentrations assumed for the monitored watersheds excluding the most polluted Cosia and Breggia basins, obtaining discharges as for the minor monitored watersheds.

2.4. Available data and preliminary analyses

Hydrological delineation of the watersheds of the tributaries to Lake Como (Fig. 1a) was performed through GIS techniques, employing the HELIDEM HD-2 (HELI-DEM, 2013; Biagi et al., 2016) cross-border Digital Terrain Model (DTM) with ~20 m resolution. This dataset harmonises the DTMs produced by Italian and Swiss governmental institutions across the alpine area. The small diffuse basins were aggregated according to the lake shore on which they are located (Fig. 1a). The GIS analysis hence reported 24 watersheds, 11 monitored and 13 unmonitored. The latters include the 5 diffuse basins. The mean slopes of the watersheds S_m were also computed from the DTM.

Land use analysis on the watersheds (Fig. 1b) was performed through the CORINE Land Cover (CLC) 2018 v.2020_20u1 raster with 100 m resolution (Copernicus, 2020), developed by the Copernicus EU programme. The 27 land uses present in the area were assembled into 8 groups (Fig. 1b), the "Urban areas" group being considered to compute the urban ratio R_u of the tributary watersheds.

In this work, we estimated total daily nutrient loads released into Lake Como by their tributary watersheds in the 2000–2019 period. Work was then performed on the available water discharge and nutrient concentration data to obtain the desired daily series.

Discharge data available for the 11 monitored basins are strongly heterogeneous:

1) for River Adda, mean daily 2000–2019 discharges were available at the Fuentes (Fig. 1a) station (ARPA Lombardia, 2022);
2) for River Mera, mean daily 2019 discharges were available at the Sorico (Fig. 1a) station (ARPA Lombardia, *unpublished data*);
3) for the monitored minor tributaries (Breggia, Caldone, Cosia, Esino, Pioverna, Rio Torto, Sanagra, Telo, Varrone), only instantaneous measurements generally performed simultaneously with chemical sampling were available, with an at best monthly resolution and

several gaps in the series, in some cases spanning multiple years (ARPA Lombardia, *unpublished data*).

To obtain mean daily discharges for River Mera for the 2000–2018 period, a linear regression against River Adda discharges was determined over the 2019 year of common availability, yielding $r = 0.848$ ($p < 0.001$):

$$Q_{Mera} = 0.383 Q_{Adda} - 1.050 \qquad (7)$$

This approach is legitimised by the similar morphoclimatic features of the Adda and Mera watersheds. As regards the minor monitored tributaries, available discharge measurements were too sparse to be interpolated. For them and for the unmonitored tributaries, reference was still made to the Adda complete series. However, due to the different morphoclimatic features of their watersheds compared to the Adda and Mera ones, relative liquid inflows with respect to the Adda watershed were estimated from the annual values given by the BIGBANG v4.0 hydrological model of the Italian Institute for Environmental Protection and Research (ISPRA) (Braca et al., 2021). The BIGBANG model, fed with observed meteorological data, computes the components of the hydrological balance for the Italian territory over a regular grid with 1 km resolution. Results are available for the 1951–2019 period (ISPRA, 2021). Liquid inflows were used instead of rainfall due to the presence of glaciers in the Adda and Mera basins (Fig. 1b), so that snow falling over them must be excluded from calculations, yet a proper estimation of annual snowmelt should be included. Baseflow estimations are not available in BIGBANG, so that the provided surface runoff variable cannot be used to estimate discharges, being only a part of the flows reaching the lake.

Annual mean liquid inflow heights were computed for all watersheds for each year of the 2000–2019 period by spatial averaging. For the Adda, Mera and Breggia basins, which partially lie in Switzerland, mean values computed on their Italian fraction were assumed for the entire watershed. Ratios between the annual mean discharges of the other watersheds and those of the Adda basin were computed from the relative annual liquid inflows and surface areas as:

$$\frac{Q_{a,i}}{Q_{a,Adda}} = \frac{I_{a,i}}{I_{a,Adda}} \frac{A_i}{A_{Adda}} \qquad (8)$$

where i is the generic watershed, Q_a is the annual mean discharge, I_a the annual mean liquid inflow and A the watershed surface area. The hypothesis behind Eq. (8) is that, on a yearly basis, the runoff coefficient can be assumed equal for all the Lake Como tributary watersheds, also due to the lag between infiltration and baseflow occurring in large part with smaller time scales. These annual ratios were then interpolated at a monthly scale and then multiplied by the monthly mean discharges observed for River Adda. Daily values were finally computed by interpolation. Liquid inflows at monthly resolution are available from BIG-BANG. However, their use led to overestimated winter discharges for the minor tributaries if they were included into Eq. (8). In fact, minor tributaries have in winter much larger liquid inflow heights than the Adda basin, for which a significant part of winter precipitation occurs in solid form. Nevertheless, winter discharges of River Adda are supported by baseflow originating from liquid rainfalls occurring during the previous months. This compensation justifies the multiplication of the monthly interpolated results of Eq. (8) by the monthly discharges of River Adda. A verification of this discharge estimation method for River Mera with respect to the 2000–2019 series produced for this main tributary led to a $-3.2\% \pm 6.9\%$ mean difference in the mean monthly discharges (a $+ 2.1\% \pm 7.4\%$ difference results for 2019, for which observations are available for River Mera).

Discrete concentration series of nitrate (*N-NO₃*), ammonium (*N-NH₄*), total nitrogen (*TN*), orthophosphate (*P-PO₄*), total phosphorus (*TP*) and conductivity at standard 20 °C conditions (*Cond*) were available from the institutional sampling activities for the monitored basins (ARPA Lombardia, *unpublished data*). As for the usually simultaneous

discharge measurements, resolution is at best monthly, with several gaps. Conductivity, being a proxy of the total dissolved ion concentration, was included to test if the proposed method worked for such variable as well. Significant trends in measured concentrations relative to measured discharges were not identified for any monitored tributary, so that it was possible to build $Q - C$ relationships valid for the whole 2000–2019 study period. This is mainly due to restoration measures on the watersheds to revert lake eutrophication having been implemented for Lake Como in the 1980s and 1990s, so that after 2000 only small water quality improvements occurred on the tributaries (Salmaso et al., 2014). Furthermore, negligible changes in land use took place over the study period, inside which effects of climate change on watershed nutrient dynamics can also be overlooked due to its relatively short duration.

Table 2 reports for the monitored and unmonitored tributary watersheds of Lake Como the mean 2000–2019 discharges obtained from the available observations and the performed hydrological estimations, together with the properties obtained through the GIS analysis. Monitored basins account for 86.1% and 88.5% of the total in terms of mean annual discharge and surface area, respectively.

3. Results and Discussion

3.1. $Q - C$ relationships of monitored basins

The NLS power-law $Q - C$ regressions for the considered variables over the monitored basins led to regression coefficients ranging $-0.790 \leq r \leq -0.053$ (Table 3), thus displaying a large variability. In the case study, power-law regressions always suitably interpret the average long-term behaviour of the observations, yet in some instances they cannot represent the observed variability. This occurs when there is a larger-than-usual chaotic variability of observed concentrations within a small discharge range, such as for N-NO_3 for Creek Rio Torto (Fig. 3b), which leads to the second worst observed r coefficient. Such variability

Table 2

Mean 2000–2019 discharges obtained from the available observations and the performed hydrological estimations and properties obtained through the GIS analysis for the monitored and unmonitored tributary watersheds of Lake Como (basins are listed by decreasing mean discharges and their abbreviations are given in parentheses).

Basin	Q_m [m³/s]	A [km²]	S_m [%]	R_u [%]
Adda (AD)	90.3	2615.0	58.9	2.1
Mera (ME)	33.5	741.0	66.4	1.6
Pioverna (PI)	8.0	157.0	58.3	4.2
Breggia (B)	4.0	86.9	40.0	21.2
Varrone (VA)	4.0	84.0	72.8	0.5
Rio Torto (RT)	3.5	77.3	23.9	23.5
Telo (T)	1.6	33.8	44.0	9.7
Cosia (CO)	1.5	33.4	37.0	25.0
Caldone (CA)	1.3	26.8	61.0	9.3
Sanagra (S)	1.1	22.4	56.5	3.8
Esino (E)	1.0	20.0	53.9	4.0
Diffuse East external (DEE)	3.5	76.0	53.4	11.5
Diffuse South-West external (DSWE)	3.2	67.5	61.9	12.7
Liro (L)	2.9	57.1	63.0	0.5
Diffuse North-West external (DNWE)	2.7	55.4	53.4	12.5
Diffuse West internal (DWI)	2.5	53.2	61.7	8.0
Albano (AL)	2.4	45.9	63.8	1.1
Val di Livo (VL)	2.3	46.6	69.6	0.4
Nosè (N)	1.3	27.0	46.2	1.0
Diffuse East internal (DEI)	1.3	27.2	55.6	15.9
Meria (MI)	1.0	21.3	80.7	4.1
Perlo (PE)	0.5	11.2	39.5	2.2
Gerenzone (G)	0.4	8.2	63.1	13.3
Zerbo (Z)	0.4	7.7	56.8	2.2
Total	174.0	4402.1	59.2	3.7

Table 3

Regression coefficients of the NLS $Q - C$ power-law regressions for the considered variables on the monitored watersheds (basins are listed by decreasing mean discharges and their abbreviations are given in parentheses; regressions with $p > 0.05$ are in italics; sample size is given in brackets).

Basin	r					
	Cond	*N-NO₃*	*N-NH₄*	*TN*	*P-PO₄*	*TP*
Adda (AD)	−0.752	−0.644	−0.615	−0.476	−0.661	−0.591
	[132]	[130]	[72]	[102]	[114]	[100]
Mera (ME)	−0.687	−0.355	−0.244	*−0.125*	*−0.146*	−0.314
	[91]	[86]	[73]	*[70]*	*[43]*	[86]
Pioverna (PI)	−0.429	−0.359	*−0.193*	−0.410	−0.437	−0.276
	[130]	[128]	*[92]*	[128]	[71]	[106]
Breggia (B)	−0.750	−0.744	*−0.502*	−0.601	*−0.378*	*−0.376*
	[14]	[13]	*[12]*	[14]	*[11]*	*[12]*
Varrone (VA)	−0.299	−0.643	*−0.192*	−0.273	−0.749	−0.319
	[119]	[124]	*[53]*	[123]	[78]	[90]
Rio Torto (RT)	−0.736	*−0.122*	−0.536	−0.397	−0.360	−0.383
	[109]	*[102]*	[103]	[107]	[97]	[103]
Telo (T)	−0.524	−0.781	*−0.299*	−0.557	−0.790	−0.645
	[27]	[28]	*[15]*	[26]	[27]	[28]
Cosia (CO)	−0.546	*−0.125*	*−0.248*	−0.392	*−0.133*	−0.433
	[47]	*[36]*	*[40]*	[42]	*[46]*	[48]
Caldone (CA)	−0.396	−0.493	−0.375	−0.378	−0.598	−0.622
	[123]	[128]	[131]	[134]	[130]	[130]
Sanagra (S)	−0.556	*−0.144*	*−0.173*	*−0.053*	−0.256	−0.219
	[134]	*[134]*	*[120]*	*[117]*	[126]	[130]
Esino (E)	−0.690	−0.688	*−0.429*	−0.684	−0.785	−0.783
	[21]	[22]	*[12]*	[21]	[22]	[22]

should be ascribed to the described complex coexisting $Q - C$ behaviours of a watershed at multiple time scales intersecting discrete institutional monitoring (Bowes et al., 2015). Small regression coefficients also result when the sample size (Table 3) is not large enough to reveal the long-term dilution behaviour, or when samples are unevenly distributed across the discharge range. When non-significant regressions with $p > 0.05$ are found (Table 3), they are mostly due to the related low r values. In some cases, such as for Creek Breggia, Creek Telo and Creek Esino (Fig. 4c), they are yet due to the insufficient sample size. The weakest regressions have been obtained for N-NH_4, limit-of-detection (LOD) issues impairing for some basins the precision of observations and reducing in others the number of available samples with respect to the other considered variables (Table 3).

Figs. 2–4 report as sample the available 2000–2019 observations and the related LLS and NLS power-law regressions for a large, a medium and a small tributary watershed, i.e. the basins of River Adda, Creek Rio Torto and Creek Esino, respectively. The NLS regressions lead to better results than the LLS ones, more properly interpolating the highest concentrations observed for the smallest discharges. In some cases, the use of a single power law for the regression shows its limits, such as for River Adda (Fig. 2), for which adopting a piecewise regression segmented at the median or mean discharge ($Q_m = 90.3$ m³/s, see Table 2), as proposed by Meybeck and Moatar (2012), would have allowed a better interpolation in the low Q – high C range through a steeper local power law. Such possibility could be evaluated in future developments of the herein introduced methodology.

3.2. $Q - C$ relationships of unmonitored basins

Transformation of the a and b coefficients of the $Q - C$ power laws obtained for the monitored basins into the $a*$ and $b*$ variables defined by Eqs. (3) and (5), respectively, led to a significant reduction of dispersion for all considered variables (Figs. 5 and 6). The NLS power-law regressions expressed by Eqs. (4) and (6) are displayed in Figs. 5 and 6. The Rio Torto basin was discarded in all regressions, the determined $a*$ and $b*$ strongly deviating from the outlined power-law trends. In the regressions of $a*$ for P-PO_4 and TP, the Breggia watershed was similarly discarded. The resulting regression coefficients are exceptionally good
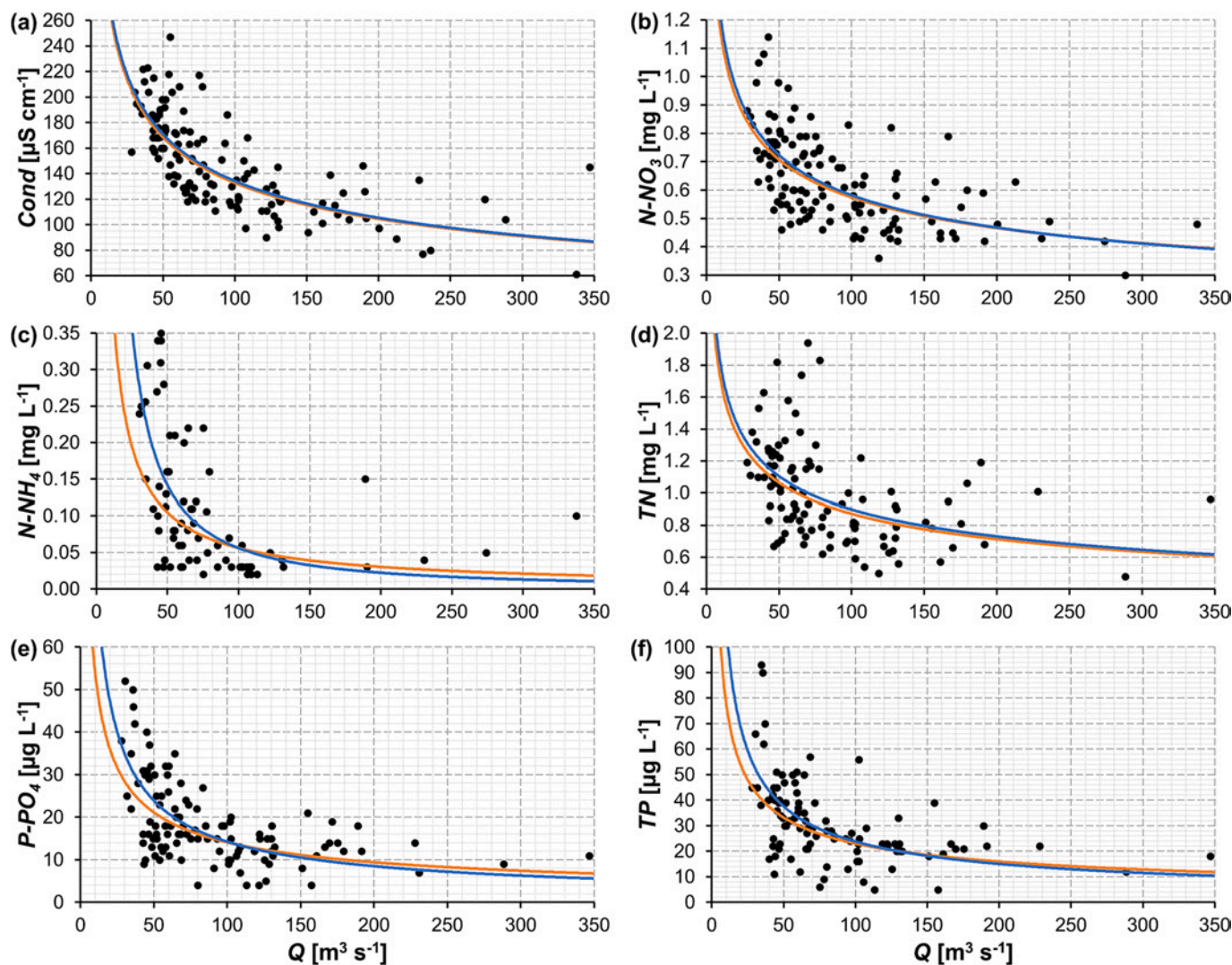
Fig. 2. $Q - C$ observations for River Adda and power-law regressions using the LLS (orange lines) and NLS (blue lines) techniques for *Cond* (a), *N-NO$_3$* (b), *N-NH$_4$* (c), *TN* (d), *P-PO$_4$* (e), *TP* (f). (For interpretation of the references to colour in this figure legend, the reader is referred to the web version of this article.)

and range $0.922 \leq r \leq 0.997$ for $a*$ and $0.797 \leq r \leq 0.978$ for $b*$ (the lower bound of the latter is 0.921 excluding *N-NO$_3$*), with $p < 0.01$ in all cases.

For $a*$, the resulting d exponents of the regressions given by Eq. (4), expressing the concavity of the curve, are $d > 1$ for all nutrient substances, describing an exponential increase of nutrient concentrations with R_u (Fig. 5b – 5f). For *Cond*, $0 < d < 1$ results instead, delineating an asymptotical stabilisation with R_u (Fig. 5a). The constant terms are all $e > 0$, complying with the physical meaning of such term. For what concerns $b*$, the obtained exponents of the regressions given in Eq. (6) are all $g < -1$. This implies an asymptotical rise of $b*$ for increasing S_m towards the threshold value given by the h constant term (Fig. 6). For the latter, very small $h < 0$ values were obtained in all cases, still complying with the physical meaning of the term.

As regards $a*$, the anomaly of the Rio Torto watershed is given by the low observed concentrations, leading to low $a*$ coefficients (Fig. 5), in relation to the high R_u of the basin (Table 2; Fig. 1b). This should be ascribed to Lake Annone, placed 3.9 km upstream of the outlet of Creek Rio Torto into Lake Como (Fig. 1a), altering the ordinary $Q - C$ dynamics (Botter et al., 2019) by abating nutrient and solute loads. A similarly noticeable behaviour is not observed for River Mera, which flows out of Lake Mezzola 3.3 km upstream of the final outlet into Lake Como (Fig. 1a). This should be first due to the Rio Torto watershed being much

more urbanised ($R_u = 23.5\%$) than the Mera one ($R_u = 1.6\%$), so that for the former there exists a much higher abatement potential. Furthermore, Lake Mezzola has a much lower 0.2 a theoretical residence time (OLL, 2005) than the combined 1.6 a one of both Lake Annone basins (OLL, 2005), which limits abatement processes. The anomaly of the $a*$ coefficients obtained for phosphorus for the Breggia basin (Fig. 5e and 5f) is still given by lower-than-expected values in relation to the high R_u (Table 2; Fig. 1b). These originate from much smaller observed phosphorus concentrations than those of the neighbouring Cosia basin, despite the similar urban ratios ($R_u = 21.2\%$ for Breggia, $R_u = 25.0\%$ for Cosia). This singularity may have to do with 61.9% of the Breggia basin, including the Chiasso urban area, being in Switzerland (Fig. 1), in which different regulations to the Italian ones exist on phosphorus control (WWTPs, fertilizers, manure disposal; Botter et al., 2019).

For $b*$, the negative coefficients obtained for the Rio Torto basin are much closer to zero than expected from its very low mean slope $S_m = 23.9\%$ (Fig. 6), which is the lowest among the monitored and unmonitored watersheds (Table 2). This slope is only marginally distorted towards lower values by Lake Annone, being a horizontal surface in the DTM, the value excluding it being $S_m = 25.7\%$. Rather, the main cause of the $b*$ anomaly is given by Lake Annone, which occupies 7.1% of the Rio Torto watershed, working as a damper of solute concentration variations, thus establishing a much more chemostatic behaviour than the
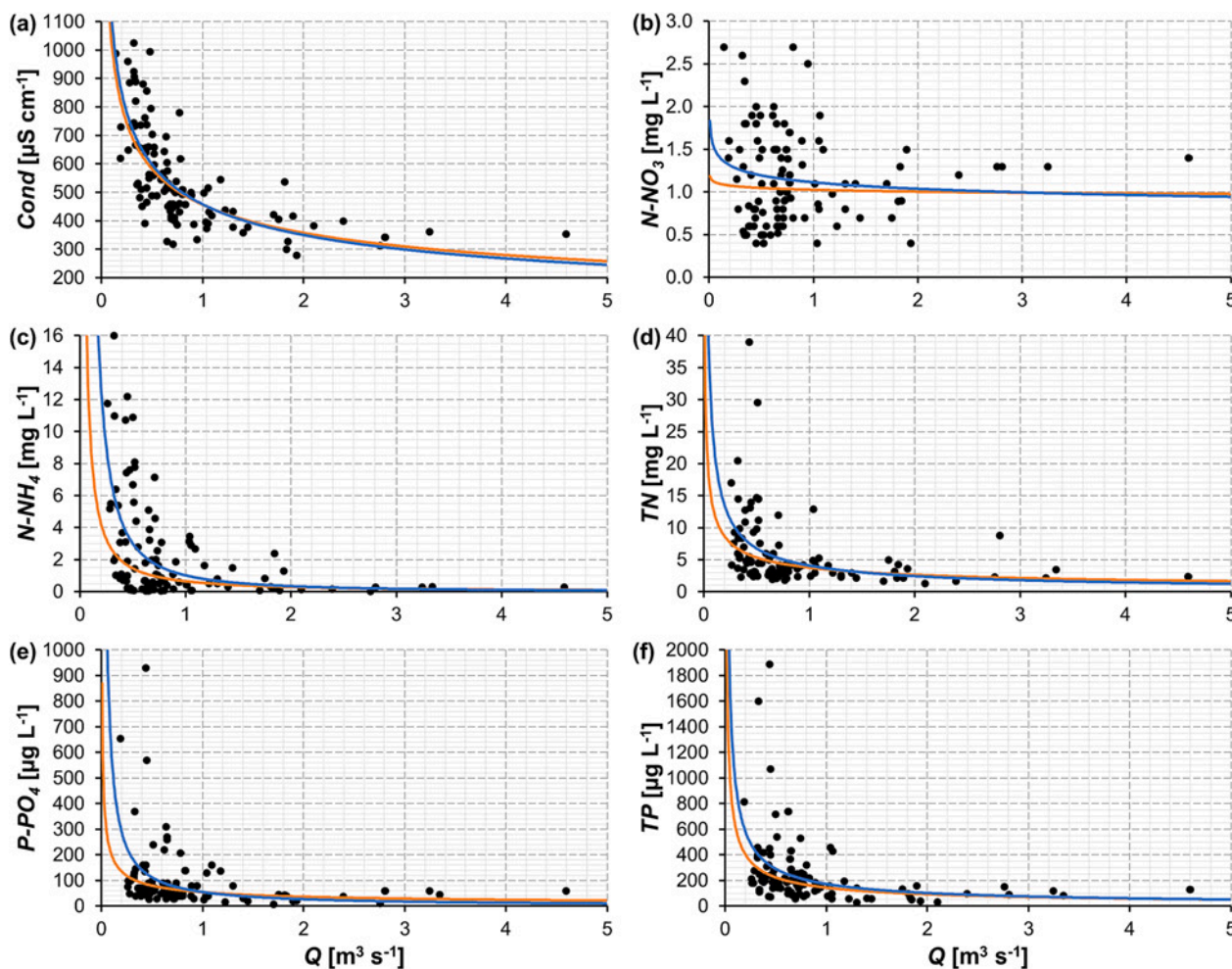
Fig. 3. $Q - C$ observations for Creek Rio Torto and power-law regressions using the LLS (orange lines) and NLS (blue lines) techniques for *Cond* (a), *N-NO₃* (b), *N-NH₄* (c), *TN* (d), *P-PO₄* (e), *TP* (f). (For interpretation of the references to colour in this figure legend, the reader is referred to the web version of this article.)

one determined by the surrounding basin. This behaviour is not clearly discernible again for the Mera basin, due to the much smaller residence time of Lake Mezzola, which furthermore occupies only 0.7% of the watershed, hence strongly limiting its damping potential.

When computing the *a* and *b* coefficients of the unmonitored basins, the cases in which extrapolations outside the ranges of the hydro-morphological parameters Q_m, S_m and R_u given for the monitored watersheds were performed are few and of small entity (3 instances for Q_m, 1 for S_m and R_u), thus limiting possible side effects. The plots of the *a* and *b* coefficients obtained for the unmonitored basins against R_u and S_m, respectively, are displayed in Fig. 7. Moderately high *a* coefficients result for the diffuse and for the Gerenzone basins due to their significant urbanisation (the latter flows through the Lecco urban area, see Fig. 1), leading to high nutrient concentrations. Very low *b* values resulted for the Liro, Nosè, Perlo and Val di Livo watersheds, below the range obtained for the monitored basins. This is due to the very low R_u of such basins not being balanced by very high S_m, thus determining a markedly chemodynamic behaviour (Eqs. (5) and (6)). On the opposite side, the diffuse and Gerenzone basins, due to their high R_u and moderately high S_m, are characterised by *b* values close to zero. For the Liro and Val di Livo basins, the very low *b* values also lead to high *a* values, given the dependency between the two coefficients (Eq. (3)), despite their very low R_u. The herein obtained *b* coefficients are generally lower than those presented in literature studies, values $b < -1$ being obtained in some cases, with a minimum $b = -4.149$ resulting for *N-NH₄* for the Perlo watershed. However, our values, determined through NLS, are intrinsically lower than the literature ones obtained through LLS, as they

weigh more correctly the low discharge range (Figs. 2–4).

Fig. 8 depicts the relationship between S_m and R_u for all monitored and unmonitored tributary basins of Lake Como. It is evident that R_u generally decreases for increasing S_m, reflecting the land inaccessibility principle. This inverse correlation is mirrored in the *b* coefficient, given the definition of $b*$ as function of R_u adopted here (Eq. (5)) and its regression against S_m (Eq. (6)), and thus also influences the *a* coefficient. The $S_m - R_u$ relationship obtained for the monitored basins is well described, excluding the Rio Torto watershed, by a further power law with constant term different from zero (Fig. 8), such as Eqs. (4) and (6), leading to $r = -0.954$ ($p < 0.001$). Unmonitored watersheds deviate more from such relationship. As a matter of fact, unmonitored basins are either small basins with very low urbanisation (Albano, Liro, Nosè, Perlo, Val di Livo, Zerbo) or diffuse basins with a very high R_u relative to S_m, consisting of the coastal towns and the mountains behind them. While for the formers low input loads are expected, justifying the lack of monitoring, the latters deliver to the lake significant nutrient masses, yet their monitoring is made extremely difficult by their diffuse nature. The Gerenzone basin shares similar $S_m - R_u$ features with the diffuse basins, leading to projected significant nutrient delivery from the Lecco urban area (Fig. 1b) according to the present estimations.

3.3. Input loads to Lake Como

Daily concentration series of *TN* and *TP* obtained from the $Q - C$ relationships estimated for monitored and unmonitored basins were corrected to avoid having *TN* values lower than *N-NO₃* + *N-NH₄*
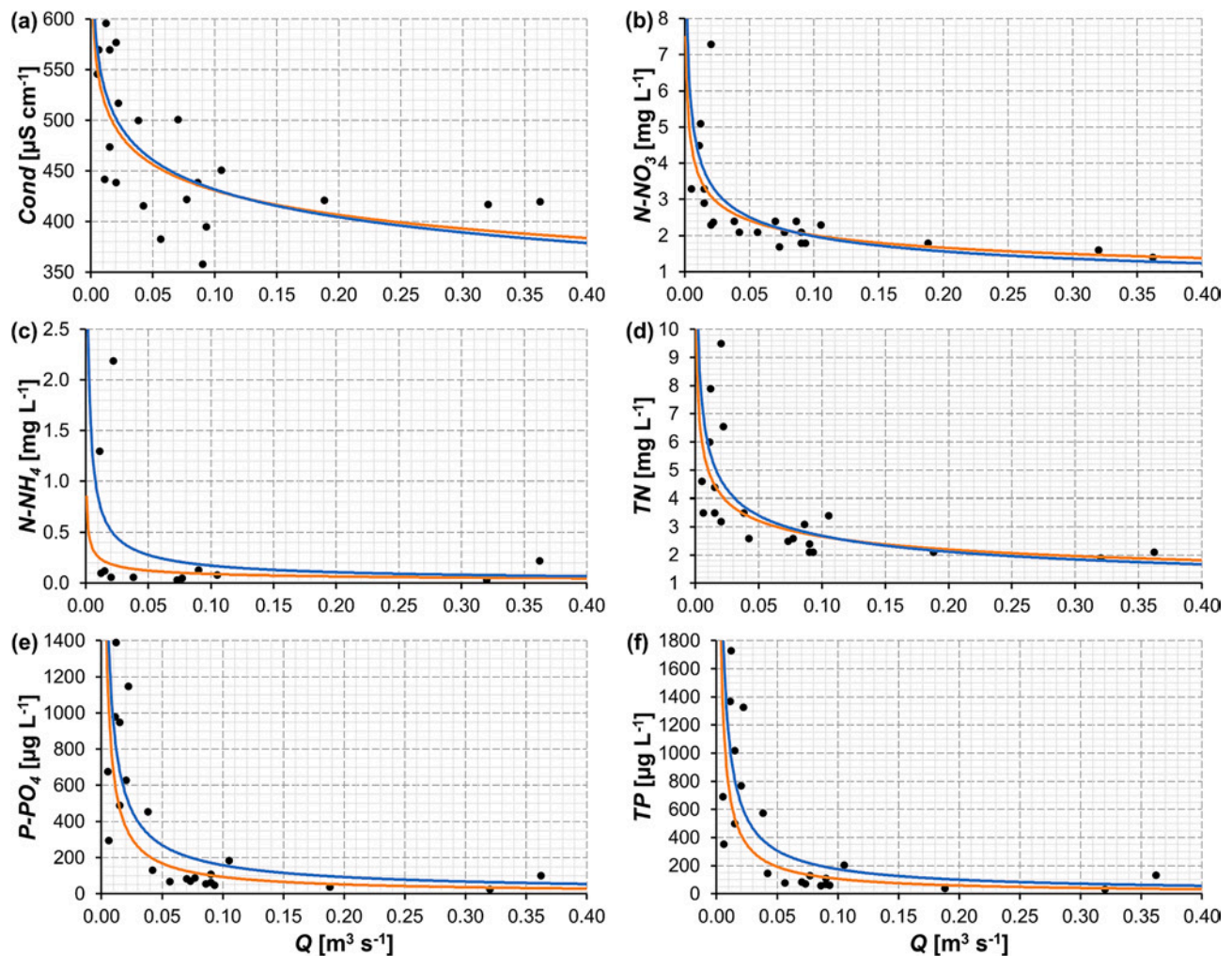
Fig. 4. $Q – C$ observations for Creek Esino and power-law regressions using the LLS (orange lines) and NLS (blue lines) techniques for *Cond* (a), *N-NO₃* (b), *N-NH₄* (c), *TN* (d), *P-PO₄* (e), *TP* (f). (For interpretation of the references to colour in this figure legend, the reader is referred to the web version of this article.)

concentrations and *TP* values lower than *P-PO₄* concentrations. These corrections involved only 3.9% and 0.9% of the overall *TN* and *TP* daily values, respectively, cumulated over all watersheds. The adjustments were necessary for 8 basins for *TN* and 3 basins for *TP* and were related to very low and/or very high discharges, for which $Q – C$ relationships are less robust due to lack of data and higher fitting uncertainty. They caused negligible 0.3% and 0.02% increases of total mean annual 2000–2019 *TN* and *TP* loads delivered to Lake Como, respectively.

The resulting total annual mean discharges $Q_{a,tot}$ and total input loads flowing into Lake Como each year for the 2000–2019 period are listed in Table 4. The total annual mean discharge has mean and standard deviation (*SD*) $Q_{m,tot} = 174.0 \pm 43.6$ m³/s over 2000–2019, thus with a relevant coefficient of variation $CV = 25.0\%$, originating from rainfall variability across years. This high variability is further highlighted by the ratio between the maximum and minimum $Q_{a,tot}$ values max/min = 2.8 obtained for the study period. The total annual loads of *N-NO₃* and *TN* follow very closely the variations of $Q_{a,tot}$, with regression coefficients $r = 0.988$ and $r = 0.993$, respectively ($p < 0.001$). This is echoed also by their barely smaller *CV* and max/min ratios than those of $Q_{a,tot}$. This behaviour is explained by the *b* values very close to zero obtained for most watersheds for *N-NO₃* and *TN* (Fig. 7b and 7d), determining an almost chemostatic behaviour. A smaller variability in terms of *CV* and max/min results for *P-PO₄* and *TP*, for which $r = 0.957$ and $r = 0.969$ regression coefficients against $Q_{a,tot}$ were attained ($p < 0.001$). This is ascribed to the higher slopes of the dilution curves

obtained for phosphorus (Fig. 7e and 7f), leading to a partial equalisation of higher discharges by smaller concentrations. For all the aforementioned solutes, the entity of loads therefore mostly depends on discharges, with a transport-limited behaviour. Interannual variability almost completely vanishes instead for *N-NH₄*, for which the lowest *b* coefficients were obtained (Fig. 7c), with $CV = 4.3\%$ and max/min = 1.2. This highlights an almost perfect chemodynamic source-limited behaviour, with a virtually constant *N-NH₄* load among years with widely different $Q_{a,tot}$. A weak, non-significant ($p > 0.05$) inverse correlation with $r = -0.190$ against $Q_{a,tot}$ is even obtained for *N-NH₄*.

The mean 2000–2019 total annual load of *TP* of 219.1 t a⁻¹ obtained here (Table 4) is 20.0% smaller than the 274 t a⁻¹ estimated nutrient emission obtained by Salerno and Buraschi (2006). This is expected, as literature export coefficients typically represent the maximum likely values for a given population or livestock unit or soil use per unit area. Considering the 2000–2004 period, the mean 227.7 t a⁻¹ *TP* load and 8368.4 t a⁻¹ *TN* load resulting from the present estimations are respectively 14.1% smaller and 6.3% larger than the mean 265 t a⁻¹ and 7871 t a⁻¹ measured nutrient loads assessed by Tartari et al. (2006) over that period. The small difference between the presently established measured nutrient loads, averaged over a 5-year base, and those determined through a more traditional approach, in which $Q – C$ dynamics were not considered, surely validates the proposed methodology. However, this also suggests that for a multi-year average the present method could not offer a superior precision, while it could be
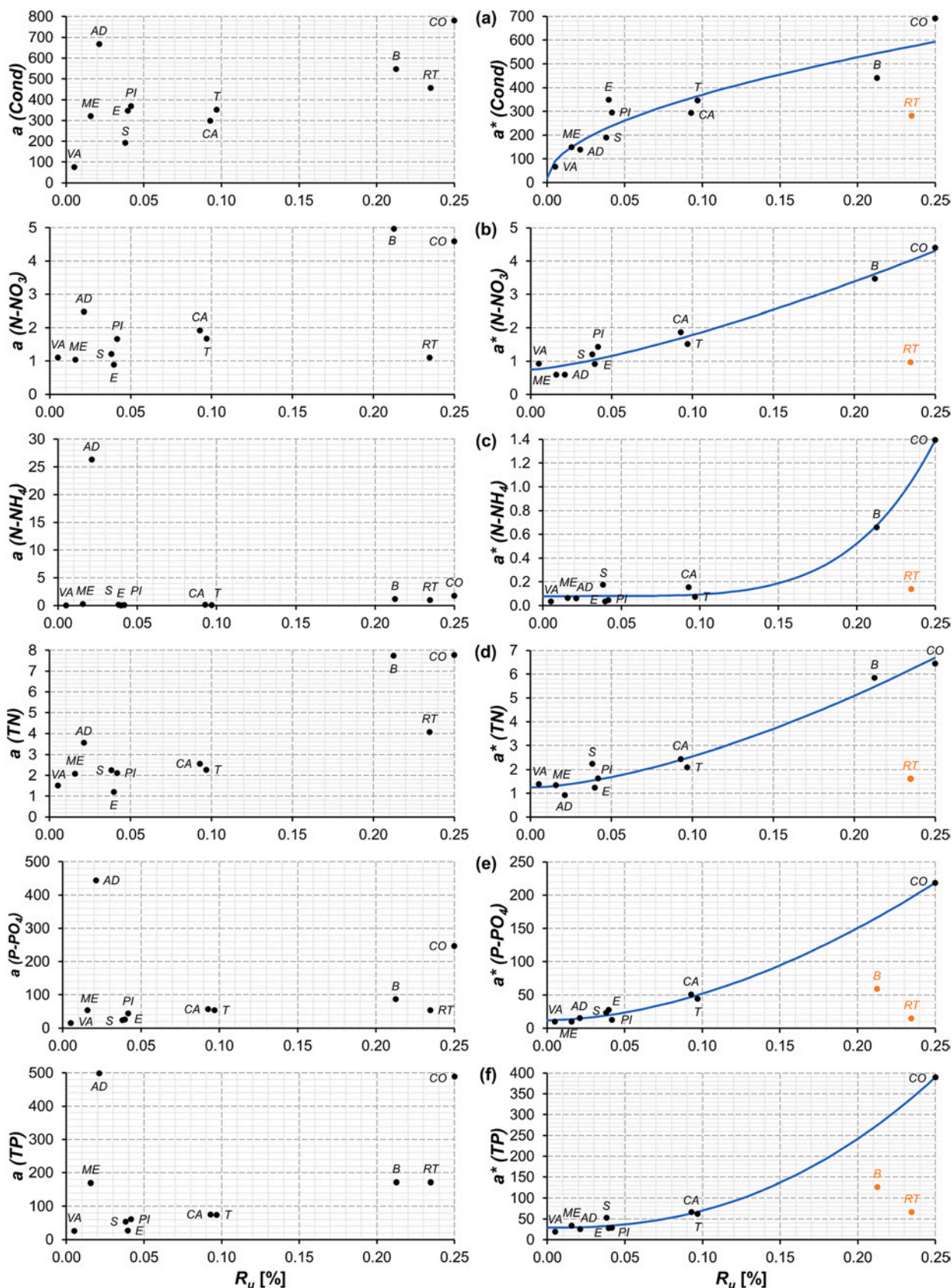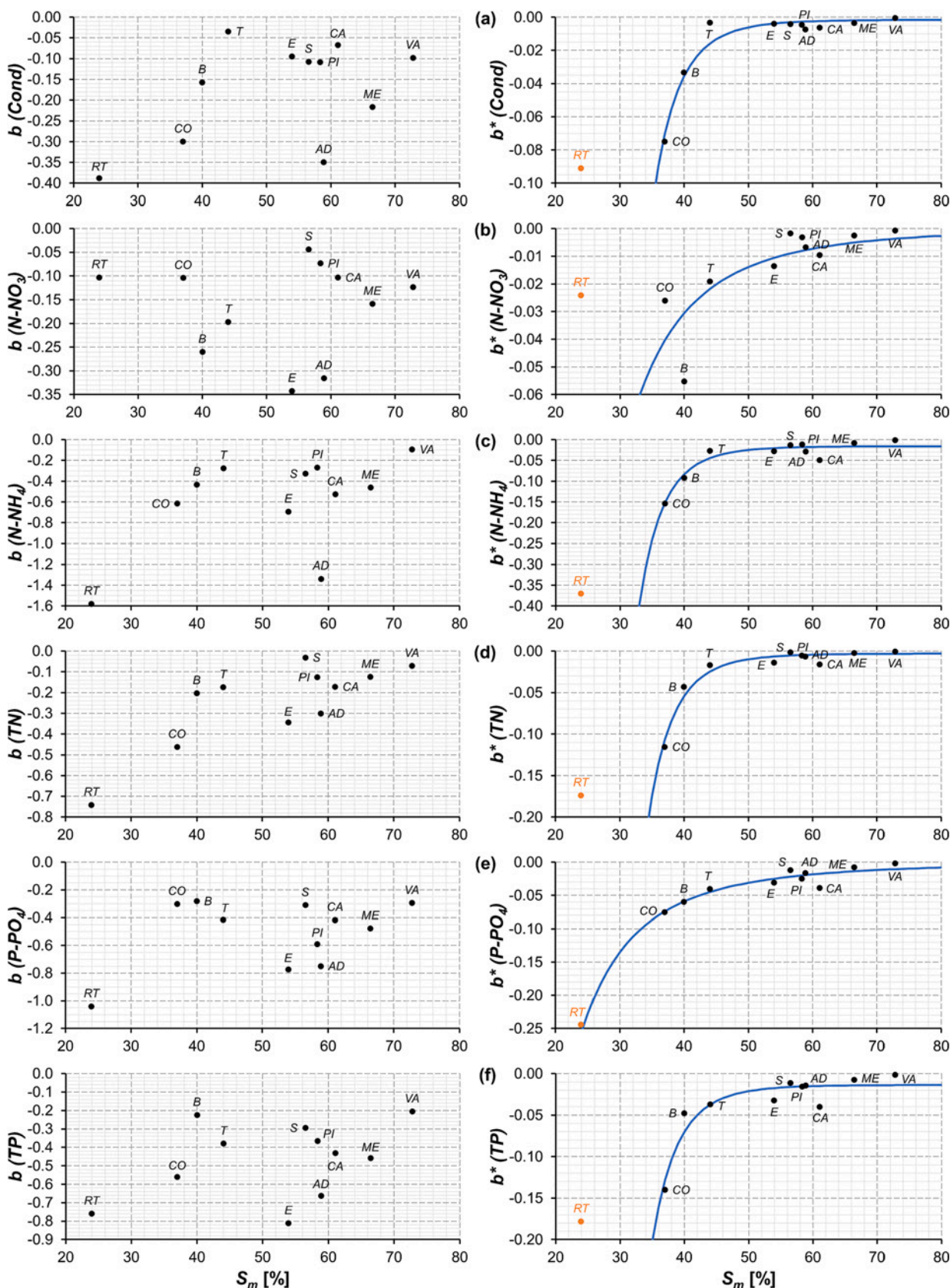
Fig. 5. Plots of the original *a* coefficients of the *Q – C* relationships and of the transformed *a** coefficients, with the related power-law regressions, against the urban ratio for the monitored basins for *Cond* (a), *N-NO₃* (b), *N-NH₄* (c), *TN* (d), *P-PO₄* (e), *TP* (f) (orange dots denote discarded basins for regression calculation; basin abbreviations are given in Table 2). (For interpretation of the references to colour in this figure legend, the reader is referred to the web version of this article.)
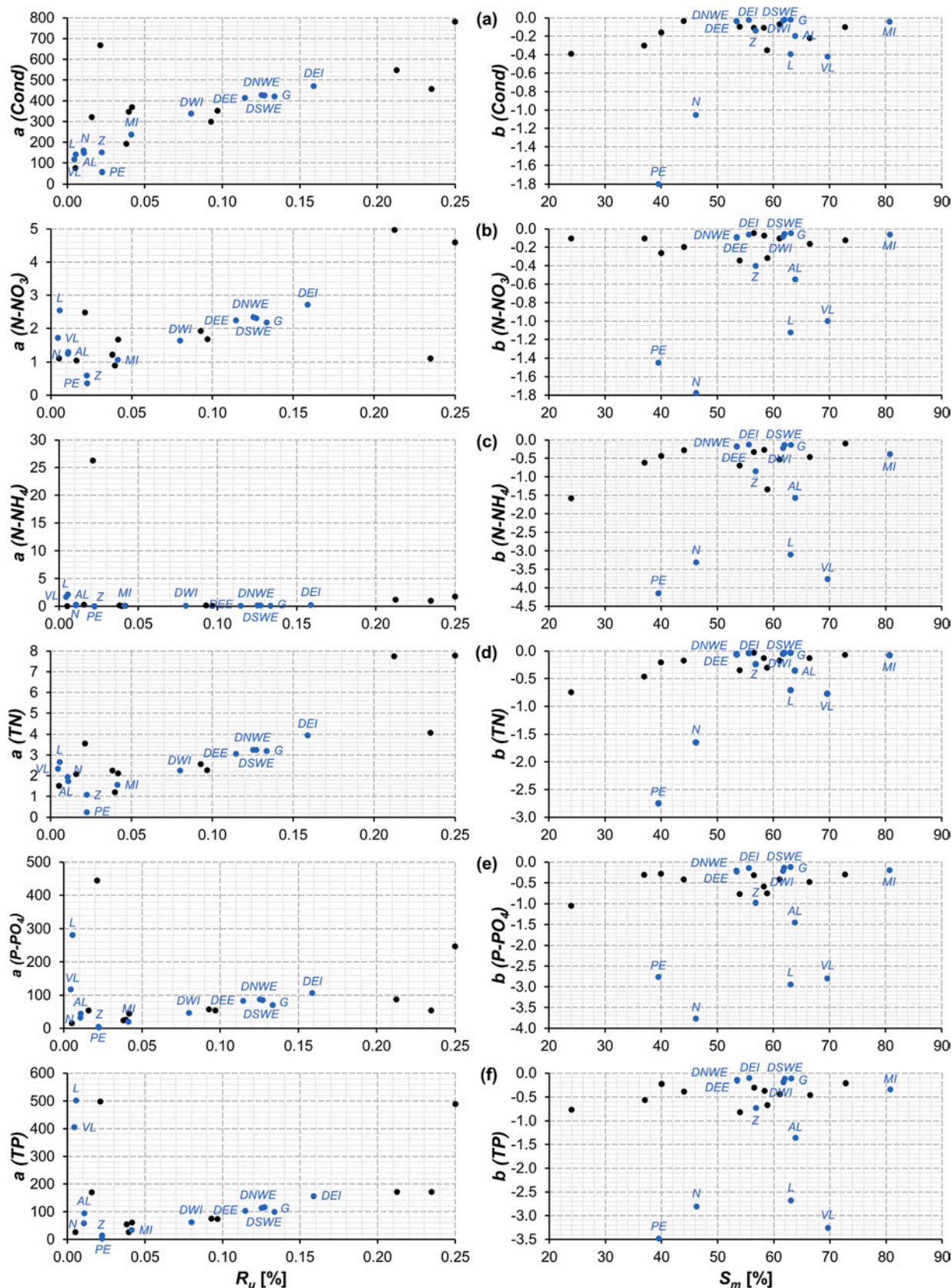
Fig. 6. Plots of the original *b* coefficients of the *Q – C* relationships and of the transformed *b** coefficients, with the related power-law regressions, against the mean slope for the monitored basins for *Cond* (a), *N-NO₃* (b), *N-NH₄* (c), *TN* (d), *P-PO₄* (e), *TP* (f) (orange dots denote discarded basins for regression calculation; basin abbreviations are given in Table 2). (For interpretation of the references to colour in this figure legend, the reader is referred to the web version of this article.)

Fig. 7. Plots of the original a and b coefficients of the $Q - C$ relationships against the urban ratio and the mean slope, respectively, for the unmonitored (blue dots, with labels) and monitored (black dots, without labels) basins for *Cond* (a), N-NO_3 (b), N-NH_4 (c), *TN* (d), P-PO_4 (e), *TP* (f) (basin abbreviations are given in Table 2). (For interpretation of the references to colour in this figure legend, the reader is referred to the web version of this article.)
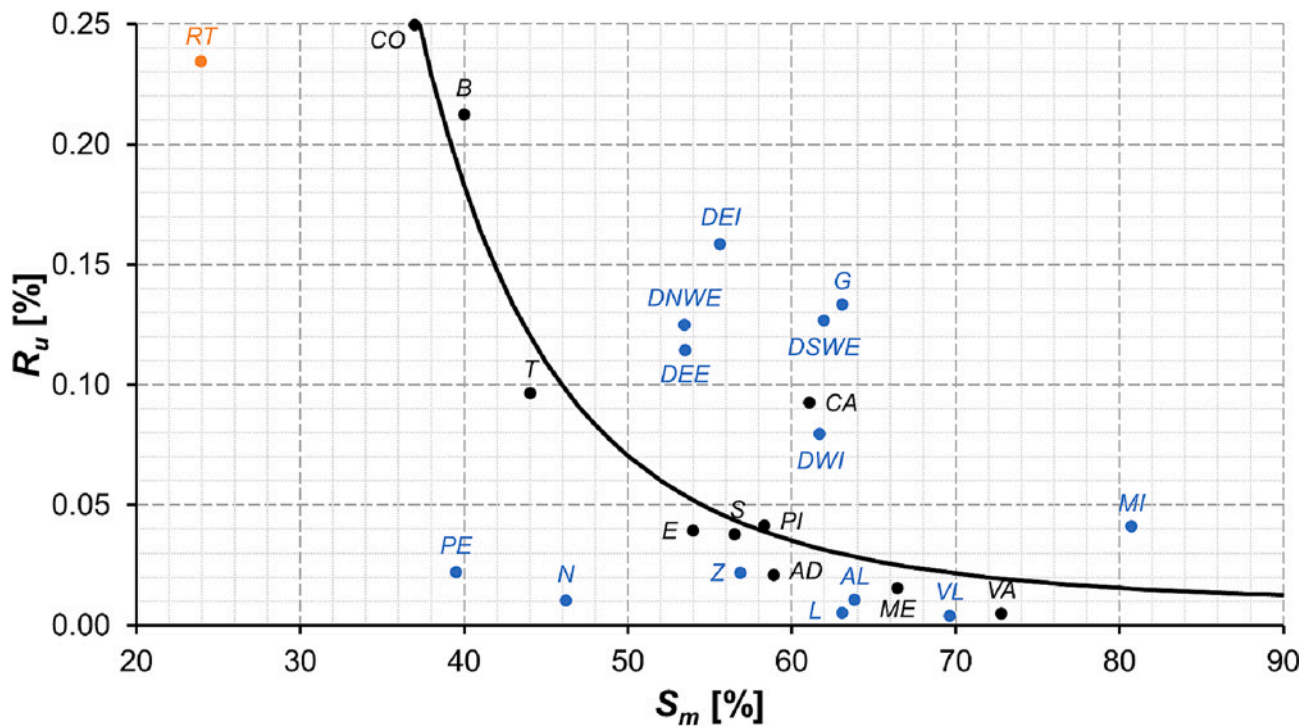
Fig. 8. Plot of the urban ratio against the mean slope for the unmonitored basins (blue dots) and for the monitored basins (black dots), for which a power-law regression is displayed, having discarded the Rio Torto watershed (orange dot) (basin abbreviations are given in Table 2). (For interpretation of the references to colour in this figure legend, the reader is referred to the web version of this article.)

Table 4

Estimated total annual mean discharges $Q_{a,tot}$ and total annual loads of the considered nutrient substances flowing into Lake Como over 2000–2019.

Annual load [t]					
Year	$Q_{a,tot}$ [m³/s]	N-NO₃	N-NH₄	TN	P-PO₄	TP
2000	236.1	6194.1	596.5	9892.3	136.3	254.2
2001	256.1	6169.4	558.3	9999.2	130.9	247.8
2002	207.3	5816.3	593.0	9180.2	132.3	243.1
2003	135.6	4004.0	563.3	6428.9	106.6	199.1
2004	131.7	3935.3	556.4	6341.3	105.3	194.5
2005	91.5	2997.1	622.0	4925.9	98.2	183.9
2006	112.3	3473.8	589.6	5641.4	101.6	189.7
2007	103.7	3313.3	598.0	5371.8	100.2	186.6
2008	176.0	4995.1	603.1	7981.8	122.4	226.8
2009	183.2	5175.9	559.5	8212.3	122.1	225.9
2010	206.0	5717.3	570.0	9039.1	129.3	238.9
2011	176.9	4787.2	524.6	7704.7	112.9	211.1
2012	185.4	4972.7	550.8	7996.3	117.2	218.8
2013	189.2	5256.2	551.0	8355.0	121.9	225.4
2014	242.2	6572.5	591.1	10389.3	142.1	262.1
2015	169.7	4819.9	548.7	7691.0	116.3	216.1
2016	166.1	4729.1	551.7	7545.3	115.1	213.7
2017	144.2	4200.3	558.1	6726.3	108.7	201.3
2018	174.1	4827.5	540.5	7703.8	114.8	214.0
2019	192.8	5338.3	560.2	8477.9	123.4	228.7
Mean ($Q_{m,tot}$) ± SD	174.0 ±43.6	4864.8 ±959.8	569.3 ±24.3	7780.2 ±1490.5	117.9 ±12.0	219.1 ±22.1
CV	25.0%	19.7%	4.3%	19.2%	10.2%	10.1%
Max/ min	2.8	2.2	1.2	2.1	1.4	1.4

significantly better at a single-year scale, or even at shorter ones, provided that more accurate hydrological estimations than the presently employed ones are included.

The mean 2000–2019 estimated loads delivered by each tributary watershed into Lake Como are reported in Table 5. While unmonitored basins contribute by 13.9% and 11.5% of the total in terms of mean annual discharge and surface area, respectively, their impact in terms of nutrient loads is greater, reaching 30.2% for $P\text{-}PO_4$, i.e. respectively 2.2 and 2.6 times larger. This is due to the highly urbanised diffuse and Gerenzone basins being among the unmonitored ones. That points out the limit of the common simplifying approach of considering nutrient loads for unmonitored basins proportional to those assessed for monitored basins on the base of discharges, or, when estimations of the latters are not available, of watershed areas, as done in the previous estimations by Tartari et al. (2006). The methodology presented here thus enables a potentially more reliable distribution of overall loads among tributary watersheds, keeping into account land use, even if presently only in terms of R_u. Actually, Tartari et al. (2006) determined for the unmonitored basins a 12.3% contribution for *TN* and a 10.9% contribution for *TP* over 2000–2004, instead of the 21.8% and 25.0% ones respectively obtained here for the same period. As a matter of fact, higher differences emerge between the present estimations and the past ones for individual basins than those presented before at the overall Lake Como watershed scale.

Mean 2000–2019 annual loads of *TN* and *TP* per unit area for all tributary basins of Lake Como are displayed in Fig. 9, in which the spatially weighted average values of 1.77 t a⁻¹ km⁻² for *TN* and 0.05 t a⁻¹ km⁻² for *TP* are also represented. The Breggia and Cosia basins stand out in terms of high *TN* unit loads, while the condition of Breggia improves greatly in terms of *TP*, as already highlighted. Among the other watersheds, the Diffuse East Internal basin emerges, being estimated to be the third and second most contaminated watershed in terms of *TN* and *TP*, respectively. Such basin includes all the municipalities on the western shore of the south-eastern arm and those on the mountains behind and is the fourth most urbanised basin after Cosia, Rio Torto and Breggia (Table 2; Fig. 1b). As a matter of fact, phytoplankton blooms have been frequently observed on that shore, ascribable to high diffuse loads (ARPA Lombardia, *personal communication*).

Another relevant basin is the Gerenzone one, which drains a portion

Table 5

Mean 2000–2019 estimated loads of the considered nutrient substances delivered to Lake Como for the monitored and unmonitored tributary watersheds (basins are listed by decreasing mean discharges and their abbreviations are given in parentheses).

Basin	Mean annual load 2000–2019 [t a^{-1}]				
	N-NO$_3$	N-NH$_4$	TN	P-PO$_4$	TP
Monitored basins					
Adda (AD)	1653.0	196.7	2549.1	42.5	69.9
Mera (ME)	622.3	66.6	1403.5	10.4	34.7
Pioverna (PI)	359.1	12.1	406.6	3.2	7.0
Breggia (B)	428.4	81.2	726.0	7.3	15.7
Varrone (VA)	115.2	4.4	171.8	1.3	2.4
Rio Torto (RT)	106.4	17.4	174.8	1.7	7.2
Telo (T)	76.3	3.8	105.1	2.2	3.1
Cosia (CO)	206.3	64.3	300.9	10.1	17.9
Caldone (CA)	78.4	6.5	101.8	2.1	2.8
Sanagra (S)	42.3	6.1	78.7	0.8	1.8
Esino (E)	26.8	1.1	36.2	0.8	0.8
Unmonitored basins					
Diffuse East external (DEE)	215.7	11.6	309.6	6.7	9.2
Diffuse South-West external (DSWE)	216.8	12.6	312.2	7.2	10.0
Liro (L)	71.8	15.5	118.7	2.2	4.5
Diffuse North-West external (DNWE)	179.2	10.3	258.2	5.9	8.2
Diffuse West internal (DWI)	117.6	6.5	168.0	3.0	4.1
Albano (AL)	58.7	6.7	94.6	1.0	2.3
Val di Livo (VL)	54.2	18.1	95.1	1.6	4.8
Nosè (N)	38.5	7.8	59.7	1.7	2.2
Diffuse East internal (DEI)	109.1	9.0	160.1	4.2	6.2
Meria (MI)	34.5	2.5	50.9	0.6	1.1
Perlo (PE)	16.4	6.1	43.0	0.5	1.4
Gerenzone (G)	27.6	1.7	39.9	0.9	1.3
Zerbo (Z)	10.1	0.9	15.7	0.2	0.3
	Fraction of the total mean annual load 2000–2019 [%]				
Monitored basins	76.4	80.8	77.8	69.8	74.6
Unmonitored basins	23.6	19.2	22.2	30.2	25.4

of the Lecco urban area (Fig. 1b), estimated to be the fourth most contaminated watershed in terms of both *TN* and *TP* unit loads. This projection is however not confirmed by visual observations, the waters of Creek Gerenzone being much clearer than those of Creek Caldone (ARPA Lombardia, *personal communication*), the other urban stream of the Lecco city (Fig. 1). The main reason for this likely mismatch should be the alteration done by the sewer network on the natural slope-based drainage assumed by the GIS watershed delineation. Differences between natural and actual watersheds are common in urban areas and should be carefully considered by future studies. This is especially relevant for unmonitored basins, for which anomalies cannot be detected, as we have done here for example for the monitored Rio Torto and Breggia watersheds.

The nutrient load abatement operated by Lake Annone is clear from Fig. 9. Despite the Rio Torto basin being the second most urbanised one (Table 2), it is far from being the most contaminated watershed in terms of unit loads of *TN* and *TP*. It is worth highlighting that the Adda basin, which leads to Lake Como by far the largest nutrient loads (Table 5) due to its prevailing size, results in the smallest unit loads of *TN* and *TP*, far smaller than the average ones of the whole lake watershed. The other major Mera tributary basin is also among the least contaminated ones.

3.4. Achievements and limitations of the present study

Regionalisation methods have long been applied in hydrology for rainfall and discharge estimations. However, to the knowledge of the Authors, this is the first time that a methodology based on ecohydrological principles is proposed to extend the regionalisation concept to nutrient load estimations. Results obtained by developing such

techniques would be strongly beneficial to the environmental management of watersheds, nutrient budgeting being one of its core needs, especially when water bodies vulnerable to eutrophication are involved. In addition, ecohydrological regionalisation methods would provide data to be used as input of water quality models or as comparison against other techniques to obtain nutrient loads in unmonitored basins. These include the estimated nutrient emission method and physically based models modelling the water-soil interaction, such as the Soil & Water Assessment Tool (SWAT+) model (SWAT, 2023). Development of eco-hydrological regionalisation methods is therefore supported, being based on actual observations on neighbouring watersheds, opposite to the literature-based estimated nutrient emission method. Furthermore, they are of relatively straightforward application and do not involve building a full coupled hydrological-ecological watershed model, such as SWAT + applications.

The proposed methodology has shown good results in the present application to the Lake Como watershed. The obtained results are overall in line with those obtained from previous estimations based on traditional techniques. Anomalies of individual monitored basins with respect to the trends identified for the transformed $a*$ and $b*$ coefficients could here be explained by physical motivations. Anomalies of unmonitored watersheds, such as the one foreseen for the Gerenzone basin, cannot be detected as easily. In such cases, discussing results with local experts could be the only way to avoid errors. Application to other case studies, being both basins of other subalpine lakes, sharing many features with the Lake Como watershed, and completely different basins, would be compelling. It would allow first evaluating the applicability range of the proposed methodology and then studying the generalisability of the regressions between hydromorphological parameters and the transformed $a*$ and $b*$ coefficients, defining the boundaries of the regionalisation approach. Validation studies involving measurements on unmonitored basins for which the $Q – C$ curves have been forecasted, including those of the present Lake Como case, would also be strongly beneficial.

This work is a first step towards the development of a thorough ecohydrological regionalisation method for nutrient and solute loads and has high margins of improvement. This is evident in the formulation of the $b*$ coefficient, for which the simplest possible approach was chosen (Eq. (5)). Future studies should also more properly investigate the influence of different land uses, only the urban ratio R_u having been employed here. For the case study, replacing R_u in Eqs. (4) and (5) with a linear combination $R_{u+a} = R_u + \alpha R_a$, where R_a is the agricultural ratio and α is a coefficient to be optimised for each substance and equation, did not lead to a significant improvement in the regression coefficients of $a*$ and $b*$. The agricultural ratio was evaluated including both the "Farmed areas" and the "Pastures and scattered cultivations" groups in Fig. 1b, weighting the latter by 0.5. Furthermore, some resulting optimal α values were hardly explicable. This may be due to the predominance of urban point sources over diffuse agricultural ones for the case study, in addition to the good correlation between R_u and R_a for the monitored basins, returning $r = 0.525$ ($r = 0.462$ including all tributary watersheds; $p < 0.05$ in both cases). In all future developments, conflicting benefits of simplicity and accuracy should always be carefully evaluated. The proposed method refers to long-term $Q – C$ curves, such as those obtained from long-term discrete monitoring data series available from environmental protection institutions. Availability of HFM monitoring data would allow evaluating ecohydrological regionalisation methods in the short term as well, suggesting specific improvements.

4. Conclusions

In this study, a method functional to the generation of continuous series of nutrient loads for monitored and neighbouring unmonitored basins, based on discrete monitoring data obtained from environmental protection institutions, has been presented. The approach exploits the power-law $Q – C$ curves obtained for the monitored basins to extract
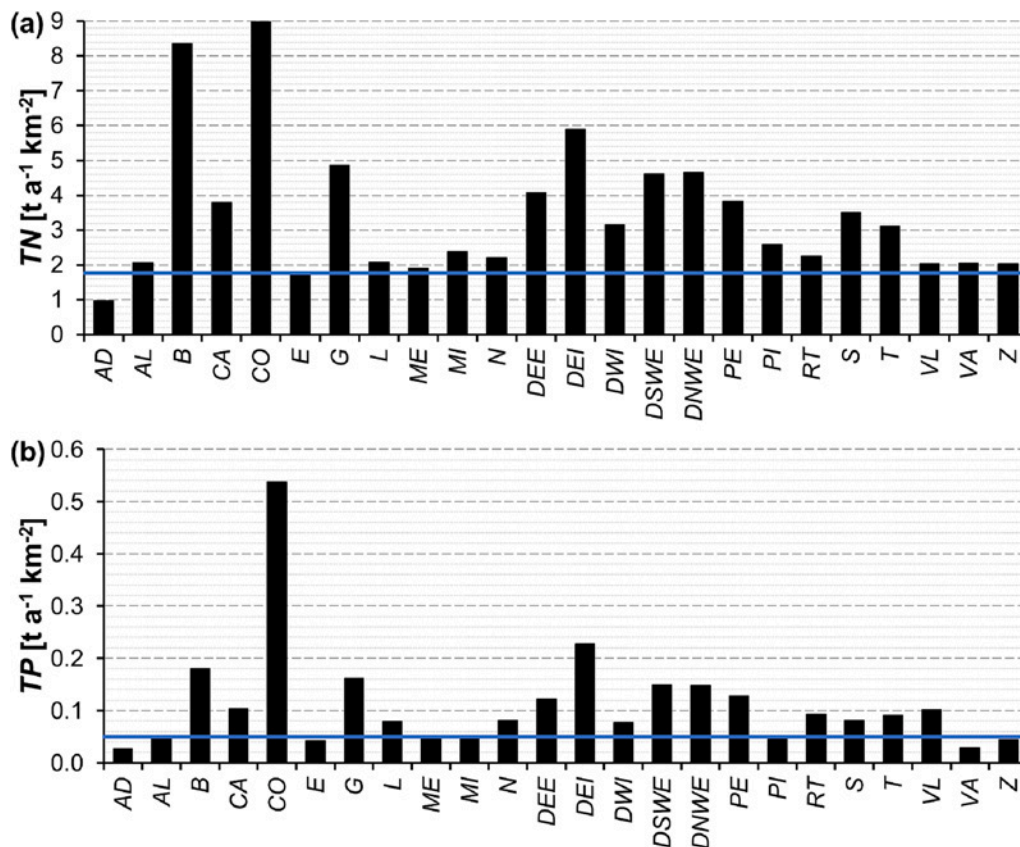
Fig. 9. Estimated 2000–2019 mean annual input loads of *TN* (a) and *TP* (b) per unit area from the tributary basins delivered to Lake Como and related average values over the whole lake watershed (blue lines) (basin abbreviations are given in Table 2). (For interpretation of the references to colour in this figure legend, the reader is referred to the web version of this article.)

trends of properly transformed power-law coefficients with respect to watershed hydromorphological parameters and infer the $Q - C$ curves of the unmonitored basins. This work represents a first step in the development of ecohydrological regionalisation techniques for the estimation of nutrient and solute loads. Application to the Lake Como watershed case study over the 2000–2019 period gave promising results and allowed evaluating the interannual variability of total nutrient loads with yearly precipitation, something which is not possible with the estimated nutrient emission method, which assumes constant export coefficients based on population equivalent and land use taken from literature.

CRediT authorship contribution statement

Andrea Fenocchi: Conceptualization, Formal analysis, Funding acquisition, Investigation, Methodology, Software, Visualization, Writing – original draft, Writing – review & editing. **Fabio Buzzi:** Data curation, Validation, Writing – review & editing. **Claudia Dresti:** Funding acquisition, Project administration, Writing – review & editing. **Diego Copetti:** Conceptualization, Formal analysis, Funding acquisition, Investigation, Supervision, Writing – review & editing.

Declaration of Competing Interest

The authors declare that they have no known competing financial interests or personal relationships that could have appeared to influence the work reported in this paper.

Data availability

Data will be made available on request.

References

Abbott, B.W., Gruau, G., Zarnetske, J.P., Moatar, F., Barbe, L., Thomas, Z., Fovet, O., Kolbe, T., Gu, S., Pierson-Wickmann, A.-C., Davy, P., Pinay, G., Grover, J., 2018. Unexpected spatial stability of water chemistry in headwater stream networks. Ecol. Lett. 21 (2), 296–308.

Arthur, S., Ashley, R.M., 1998. The influence of near bed solids transport on first foul flush in combined sewers. Water Sci. Technol. 37 (1), 131–138. https://doi.org/10.1016/S0273-1223(97)00762-2.

Asselman, N.E.M., 2000. Fitting and interpretation of sediment rating curves. J. Hydrol. 234 (3–4), 228–248. https://doi.org/10.1016/S0022-1694(00)00253-5.

Balerna, J.A., Melone, J.C., Knee, K.L., 2021. Using concentration–discharge relationships to identify influences on surface and subsurface water chemistry along a watershed urbanization gradient. Water 13 (5), 662. https://doi.org/10.3390/w13050662.

Basu, N.B., Thompson, S.E., Rao, P.S.C., 2011. Hydrologic and biogeochemical functioning of intensively managed catchments: a synthesis of top-down analyses. Water Resour. Res. 47 (10), W00J15. https://doi.org/10.1029/2011WR010800.

Behrendt, H., 1996. Inventories of point and diffuse sources and estimated nutrient loads – A comparison for different river basins in Central Europe. Water Sci. Technol. 33 (4–5), 99–107. https://doi.org/10.1016/0273-1223(96)00219-3.

Bergner, F., Zouhar, G., 2000. A new approach to the correlation between the coefficient and the exponent in the power law equation of fatigue crack growth. Int. J. Fatigue 22 (3), 229–239. https://doi.org/10.1016/S0142-1123(99)00123-1.

Bettinetti, R., Morabito, G., Provini, A., 2000. Phytoplankton assemblage structure and dynamics as indicator of the recent trophic and biological evolution of the western basin of Lake Como (N. Italy). Hydrobiologia 435, 177–190. https://doi.org/10.1023/A:1004055710353.

Biagi, L., Caldera, S., Carcano, L., Negretti, M., 2016. The open data HELI-DEM DTM for the western alpine area: computation and publication. Appl. Geomat. 8, 191–200. https://doi.org/10.1007/s12518-016-0176-5.

Bieroza, M.Z., Heathwaite, A.L., 2015. Seasonal variation in phosphorus concentration–discharge hysteresis inferred from high-frequency in situ monitoring. J. Hydrol. 524, 333–347. https://doi.org/10.1016/j.jhydrol.2015.02.036.

Bieroza, M.Z., Heathwaite, A.L., Bechmann, M., Kyllmar, K., Jordan, P., 2018. The concentration-discharge slope as a tool for water quality management. Sci. Total Environ. 630, 738–749. https://doi.org/10.1016/j.scitotenv.2018.02.256.

Botter, M., Burlando, P., Fatichi, S., 2019. Anthropogenic and catchment characteristic signatures in the water quality of Swiss rivers: a quantitative assessment. Hydrol. Earth Syst. Sc. 23, 1885–1904. https://doi.org/10.5194/hess-23-1885-2019.

Bowes, M.J., Jarvie, H.P., Halliday, S.J., Skeffington, R.A., Wade, A.J., Loewenthal, M., Gozzard, E., Newman, J.R., Palmer-Felgate, E.J., 2015. Characterising phosphorus and nitrate inputs to a rural river using high-frequency concentration–flow relationships. Sci. Total Environ. 511, 608–620. https://doi.org/10.1016/j.scitotenv.2014.12.086.

Braca, G., Bussettini, M., Lastoria, B., Mariani, S., Piva, F., 2021. Il Bilancio Idrologico Gis BAsed a scala Nazionale su Griglia regolare – BIGBANG: metodologia e stime. Rapporto sulla disponibilità naturale della risorsa idrica (*GIS-based hydrological balance at national scale over a regular grid – BIGBANG: methodology and estimations. Report on the natural availability of the water resource*) [in Italian]. Italian Institute for Environmental Protection and Research (ISPRA), Rome. Report 339/21. https://www.isprambiente.gov.it/files2021/pubblicazioni/rapporti/rapporto_ispra_339-21_bigbang_ld.pdf (accessed 24 May 2023).

Cartwright, I., 2020. Concentration vs. streamflow (C-Q) relationships of major ions in south-eastern Australian rivers: Sources and fluxes of inorganic ions and nutrients. Appl. Geochem. 120, 104680 https://doi.org/10.1016/j.apgeochem.2020.104680.

Clauset, A., Shalizi, C.R., Newman, M.E.J., 2009. Power-law distributions in empirical data. SIAM Rev. 51 (4), 661–703. https://doi.org/10.1137/070710111.

Copernicus, 2020. CORINE Land Cover (CLC) 2018, Version 2020_20u1. https://land.copernicus.eu/pan-european/corine-land-cover/clc2018.

Copetti, D., Marziali, L., Viviano, G., Valsecchi, L., Guzzella, L., Capodaglio, A.G., Tartari, G., Polesello, S., Valsecchi, S., Mezzanotte, V., Salerno, F., 2019. Intensive monitoring of conventional and surrogate quality parameters in a highly urbanized river affected by multiple combined sewer overflows. Water Supply 19 (3), 953–966. https://doi.org/10.2166/ws.2018.146.

Copetti, D., Guyennon, N., Buzzi, F., 2020. Generation and dispersion of chemical and biological gradients in a large-deep multi-basin lake (Lake Como, north Italy): the joint effect of external drivers and internal wave motions. Sci. Total. Environ. 749, 141587 https://doi.org/10.1016/j.scitotenv.2020.141587.

D'Amario, S.C., Wilson, H.F., Xenopoulos, M.A., 2021. Concentration-discharge relationships derived from a larger regional dataset as a tool for watershed management. Ecol. Appl. 31 (8), e02447.

Gruppo di Lavoro Lago di Como, 2006. Progetto PLINIUS – Criticità e azioni per il recupero della qualità delle acque del Lario (*PLINIUS Project – Critical issues and actions for the restoration of Lake Como water quality*) [in Italian]. Centro Volta, Como.

Dralle, D., Karst, N., Thompson, S.E., 2015. a, b careful: the challenge of scale invariance for comparative analyses in power law models of the streamflow recession. Geophys. Res. Lett. 42 (21), 9285–9293. https://doi.org/10.1002/2015GL066007.

Dresti, C., Fenocchi, A., Copetti, D., 2021. Modelling physical and ecological processes in medium-to-large deep European perialpine lakes: a review. J. Limnol. 80 (3), 2041. https://doi.org/10.4081/jlimnol.2021.2041.

Duncan, J.M., Welty, C., Kemper, J.T., Groffman, P.M., Band, L.E., 2017. Dynamics of nitrate concentration-discharge patterns in an urban watershed. Water Resour. Res. 53 (8), 7349–7365. https://doi.org/10.1002/2017WR020500.

EU WFD, 2000. Directive 2000/60/EC of the European Parliament and of the Council of 23 October 2000 establishing a framework for Community action in the field of water policy. https://eur-lex.europa.eu/legal-content/EN/TXT/?uri=CELEX:32000L0060 (accessed 24 May 2023).

Fenocchi, A., Rogora, M., Morabito, G., Marchetto, A., Sibilla, S., Dresti, C., 2019. Applicability of a one-dimensional coupled ecological-hydrodynamic numerical model to future projections in a very deep large lake (Lake Maggiore, Northern Italy/Southern Switzerland). Ecol. Model. 392, 38–51. https://doi.org/10.1016/j.ecolmodel.2018.11.005.

Ferreira, J.G., Vale, C., Soares, C.V., Salas, F., Stacey, P.E., Bricker, S.B., Silva, M.C., Marques, J.C., 2007. Monitoring of coastal and transitional waters under the E.U. Water Framework Directive. Environ. Monit. Assess. 135, 195–216. https://doi.org/10.1007/s10661-007-9643-0.

Fu, B., Horsburgh, J.S., Jakeman, A.J., Gualtieri, C., Arnold, T., Marshall, L., Green, T.R., Quinn, N.W.T., Volk, M., Hunt, R.J., Vezzaro, L., Croke, B.F.W., Jakeman, J.D., Snow, V., Rashleigh, B., 2020. Modeling water quality in watersheds: from here to the next generation. Water Resour. Res. 56 (11) https://doi.org/10.1029/2020WR027721.

Godsey, S.E., Kirchner, J.W., Clow, D.W., 2009. Concentration–discharge relationships reflect chemostatic characteristics of US catchments. Hydrol. Process. 23 (13), 1844–1864. https://doi.org/10.1002/hyp.7315.

Godsey, S.E., Hartmann, J., Kirchner, J.W., 2019. Catchment chemostasis revisited: water quality responds differently to variations in weather and climate. Hydrol. Process. 33 (24), 3056–3069. https://doi.org/10.1002/hyp.13554.

Goldstein, M.L., Morris, S.A., Yen, G.G., 2004. Problems with fitting to the power-law distribution. Eur. Phys. J. B 41, 255–258. https://doi.org/10.1140/epjb/e2004-00316-5.

Guo, Y., Zhang, Y., Zhang, L., Wang, Z., 2021. Regionalization of hydrological modeling for predicting streamflow in ungauged catchments: a comprehensive review. WIREs Water 8 (1), e1487.

Guyennon, N., Valerio, G., Salerno, F., Pilotti, M., Tartari, G., Copetti, D., 2014. Internal wave weather heterogeneity in a deep multi-basin subalpine lake resulting from wavelet transform and numerical analysis. Adv. Water. Resour. 71, 149–161. https://doi.org/10.1016/j.advwatres.2014.06.013.

He, Y., Bárdossy, A., Zehe, E., 2011. A review of regionalisation for continuous streamflow simulation. Hydrol. Earth Syst. Sc. 15 (11), 3539–3553. https://doi.org/10.5194/hess-15-3539-2011.

HELI-DEM, 2013. DTM HELIDEM HD-2. https://data.europa.eu/data/datasets/r_piemon-2cd69990-0c8c-4a76-9ffa-0229fc4a8284.

Herndon, E.M., Dere, A.L., Sullivan, P.L., Norris, D., Reynolds, B., Brantley, S.L., 2015. Landscape heterogeneity drives contrasting concentration–discharge relationships in shale headwater catchments. Hydrol. Earth Syst. Sc. 19, 3333–3347. https://doi.org/10.5194/hess-19-3333-2015.

House, W.A., Warwick, M.S., 1998. Hysteresis of the solute concentration/discharge relationship in rivers during storms. Water Res. 32 (8), 2279–2290. https://doi.org/10.1016/S0043-1354(97)00473-9.

Ibarra, D.E., Caves, J.K., Moon, S., Thomas, D.L., Hartmann, J., Chamberlain, C.P., Maher, K., 2016. Differential weathering of basaltic and granitic catchments from concentration–discharge relationships. Geochim. Cosmochim. Ac. 190, 265–293. https://doi.org/10.1016/j.gca.2016.07.006.

ISPRA, 2021. Hydrological balance ASCII grid data given by BIGBANG v4.0 for 1951-2019. https://groupware.sinanet.isprambiente.it/bigbang-data/library/bigbang40/grids.

Janssen, A.B.G., van Wijk, D., van Gerven, L.P.A., Bakker, E.S., Brederveld, R.J., DeAngelis, D.L., Janse, J.H., Mooij, W.M., 2019. Success of lake restoration depends on spatial aspects of nutrient loading and hydrology. Sci. Total. Environ. 679, 248–259. https://doi.org/10.1016/j.scitotenv.2019.04.443.

Knapp, J.L.A., von Freyberg, J., Studer, B., Kiewiet, L., Kirchner, J.W., 2020. Concentration–discharge relationships vary among hydrological events, reflecting differences in event characteristics. Hydrol. Earth Syst. Sc. 24, 2561–2576. https://doi.org/10.5194/hess-24-2561-2020.

Lombardia, ARPA. SIDRO – Sistema Informativo Idrologico (*Hydrological Information System*). https://idro.arpalombardia.it/it/map/sidro/.

Maher, K., Chamberlain, C.P., 2014. Hydrologic regulation of chemical weathering and the geologic carbon cycle. Science 343 (6178), 1502–1504. https://doi.org/10.1126/science.1250770.

Marcé, R., George, G., Buscarinu, P., Deidda, M., Dunalska, J., de Eyto, E., Flaim, G., Grossart, H.-P., Istvanovics, V., Lenhardt, M., Moreno-Ostos, E., Obrador, B., Ostrovsky, I., Pierson, D.C., Potužák, J., Poikane, S., Rinke, K., Rodríguez-Mozaz, S., Staehr, P.A., Šumberová, K., Waajen, G., Weyhenmeyer, G.A., Weathers, K.C., Zion, M., Ibelings, B.W., Jennings, E., 2016. Automatic high frequency monitoring for improved lake and reservoir management. Environ. Sci. Technol. 50 (20), 10780–10794.

Mather, A.L., Johnson, R.L., 2014. Quantitative characterization of stream turbidity-discharge behavior using event loop shape modeling and power law parameter decorrelation. Water Resour. Res. 50 (10), 7766–7779. https://doi.org/10.1002/2014WR015417.

Meybeck, M., Moatar, F., 2012. Daily variability of river concentrations and fluxes: indicators based on the segmentation of the rating curve. Hydrol. Process. 26 (8), 1188–1207. https://doi.org/10.1002/hyp.8211.

Miller, D.M., 1984. Reducing transformation bias in curve fitting. Am. Stat. 38 (2), 124–126. https://doi.org/10.1080/00031305.1984.10483180.

Minaudo, C., Dupas, R., Gascuel-Odoux, C., Roubeix, V., Danis, P.-A., Moatar, F., 2019. Seasonal and event-based concentration-discharge relationships to identify catchment controls on nutrient export regimes. Adv. Water Resour. 131, 103379 https://doi.org/10.1016/j.advwatres.2019.103379.

Moatar, F., Abbott, B.W., Minaudo, C., Curie, F., Pinay, G., 2017. Elemental properties, hydrology, and biology interact to shape concentration-discharge curves for carbon, nutrients, sediment, and major ions. Water Resour. Res. 53 (2), 1270–1287. https://doi.org/10.1002/2016WR019635.

Moatar, F., Meybeck, M., 2005. Compared performances of different algorithms for estimating annual nutrient loads discharged by the eutrophic River Loire. Hydrol. Process. 19 (2), 429–444. https://doi.org/10.1002/hyp.5541.

Moon, S., Chamberlain, C.P., Hilley, G.E., 2014. New estimates of silicate weathering rates and their uncertainties in global rivers. Geochim. Cosmochim. Ac. 134, 257–274. https://doi.org/10.1016/j.gca.2014.02.033.

Musolff, A., Schmidt, C., Selle, B., Fleckenstein, J.H., 2015. Catchment controls on solute export. Adv. Water Resour. 86 (A), 133–146. https://doi.org/10.1016/j.advwatres.2015.09.026.

Nielsen, A., Trolle, D., Søndergaard, M., Lauridsen, T.L., Bjerring, R., Olesen, J.E., Jeppesen, E., 2012. Watershed land use effects on lake water quality in Denmark. Ecol. Appl. 22 (4), 1187–1200. https://doi.org/10.1890/11-1831.1.

Osservatorio dei Laghi Lombardi (Regione Lombardia, ARPA Lombardia, Fondazione Lombardia per l'Ambiente, CNR-IRSA), 2005. Qualità delle acque lacustri in Lombardia – 1° Rapporto OLL 2004 (*Quality of lake waters in Lombardy – 1st OLL Report 2004*) [in Italian]. Osservatorio dei Laghi Lombardi, Milan. https://www.regione.lombardia.it/wps/wcm/connect/b3037062-15c4-4d78-a464-8f7ba8935028/OLL_rapp2004_aggiornato_dicembre_2005.pdf?MOD=AJPERES&CACHEID=b3037062-15c4-4d78-a464-8f7ba8935028 (accessed 24 May 2023).

Pattyn, F., Van Huele, W., 1998. Power law or power flaw? Earth Surf. Proc. Land. 23 (8), 761–767. https://doi.org/10.1002/(SICI)1096-9837(199808)23:8<761::AID-ESP892>3.0.CO;2-K.

Rast, W., Lee, G.F., 1983. Nutrient loading estimates for lakes. J. Environ. Eng.-ASCE 109 (2), 502–517. https://doi.org/10.1061/(ASCE)0733-9372(1983)109:2(502).

Rode, M., Wade, A.J., Cohen, M.J., Hensley, R.T., Bowes, M.J., Kirchner, J.W., Arhonditsis, G.B., Jordan, P., Kronvang, B., Halliday, S.J., Skeffington, R.A., Rozemeijer, J.C., Aubert, A.H., Rinke, K., Jomaa, S., 2016. Sensors in the stream: the high-frequency wave of the present. Environ. Sci. Technol. 50 (19), 10297–10307.

Rogora, M., Buzzi, F., Dresti, C., Leoni, B., Lepori, F., Mosello, R., Patelli, M., Salmaso, N., 2018. Climatic effects on vertical mixing and deep-water oxygen content in the subalpine lakes in Italy. Hydrobiologia 842, 33–50. https://doi.org/10.1007/s10750-018-3623-y.

Salerno, F., Buraschi, E., 2006. Antropizzazione del territorio (*Anthropisation of the land*) [in Italian]. In: Gruppo di Lavoro Lago di Como (Eds.), Progetto PLINIUS – Criticità e azioni per il recupero della qualità delle acque del Lario (*PLINIUS Project – Critical issues and actions for the restoration of Lake Como water quality*). Centro, Volta, Como, pp. 59–70.

Salerno, F., Viviano, G., Tartari, G., 2018. Urbanization and climate change impacts on surface water quality: enhancing the resilience by reducing impervious surfaces. Water Res. 144, 491–502. https://doi.org/10.1016/j.watres.2018.07.058.

Salmaso, N., Mosello, R., 2010. Limnological research in the deep southern subalpine lakes: synthesis, directions and perspectives. Adv. Oceanogr. Limnol. 1 (1), 29–66. https://doi.org/10.1080/19475721003735773.

Salmaso, N., Buzzi, F., Cerasino, L., Garibaldi, L., Leoni, B., Morabito, G., Rogora, M., Simona, M., 2014. Influence of atmospheric modes of variability on the limnological characteristics of large lakes south of the Alps: a new emerging paradigm. Hydrobiologia 731, 31–48. https://doi.org/10.1007/s10750-013-1659-6.

Shanley, J.B., McDowell, W.H., Stallard, R.F., 2011. Long-term patterns and short-term dynamics of stream solutes and suspended sediment in a rapidly weathering tropical watershed. Water Resour. Res. 47 (7), W07515. https://doi.org/10.1029/2010WR009788.

Skeffington, R.A., Halliday, S.J., Wade, A.J., Bowes, M.J., Loewenthal, M., 2015. Using high-frequency water quality data to assess sampling strategies for the EU Water Framework Directive. Hydrol. Earth Syst. Sc. 19 (5), 2491–2504. https://doi.org/10.5194/hess-19-2491-2015.

SWAT, 2023. Soil & Water Assessment Tool. https://swat.tamu.edu/ (accessed 24 May 2023).

Syvitski, J.P., Morehead, M.D., Bahr, D.B., Mulder, T., 2000. Estimating fluvial sediment transport: the rating parameters. Water Resour. Res. 36 (9), 2747–2760. https://doi.org/10.1029/2000WR900133.

Tartari, G., Salerno, F., Mosello, F., Brambilla, A., 2006. In: Valutazione del carico di nutrienti dal bacino imbrifero (*Evaluation of nutrient load from the watershed*) [in Italian]. In: Gruppo di Lavoro Lago di Como (Eds.), Progetto PLINIUS – Criticità e azioni per il recupero della qualità delle acque del Lario (*PLINIUS Project – Critical issues and actions for the restoration of Lake Como water quality*). Centro, Volta, Como, pp. 91–98.

Thomas, Z., Abbott, B.W., Troccaz, O., Baudry, J., Pinay, G., 2016. Proximate and ultimate controls on carbon and nutrient dynamics of small agricultural catchments. Biogeosciences 13, 1863–1875. https://doi.org/10.5194/bg-13-1863-2016.

Thompson, S.E., Basu, N.B., Lascurain Jr., J., Aubeneau, A., Rao, P.S.C., 2011. Relative dominance of hydrologic versus biogeochemical factors on solute export across impact gradients. Water Resour. Res. 47 (10), W00J05. https://doi.org/10.1029/2010WR009605.

Tiberti, R., Caroni, R., Cannata, M., Lami, A., Manca, D., Strigaro, D., Rogora, M., 2021. Automated high frequency monitoring of Lake Maggiore through in situ sensors: system design, field test and data quality control. J. Limnol. 80 (2), 2011. https://doi.org/10.4081/jlimnol.2021.2011.

Torres, M.A., Baronas, J.J., 2021. Modulation of riverine concentration-discharge relationships by changes in the shape of the water transit time distribution. Global Biogeochem. Cy. 35(1), e2020GB006694. https://doi.org/10.1029/2020GB006694.

Torres, M.A., Baronas, J.J., Clark, K.E., Feakins, S.J., West, A.J., 2017. Mixing as a driver of temporal variations in river hydrochemistry: 1. Insights from conservative tracers in the Andes-Amazon transition. Water Resour. Res. 53(4), 3102-3119. https://doi.org/10.1002/2016WR019733.

Torres, M.A., West, A.J., Clark, K.E., 2015. Geomorphic regime modulates hydrologic control of chemical weathering in the Andes-Amazon. Geochim. Cosmochim. Ac. 166, 105–128. https://doi.org/10.1016/j.gca.2015.06.007.

Valerio, G., Pilotti, M., Scibona, A., Nizzoli, D., 2022. Monitoring phosphorus in the tributaries of a deep lake from the perspective of the receiving water body. Hydrol. Process. 36 (7), e14612.

Viviano, G., Salerno, F., Manfredi, E.C., Polesello, S., Valsecchi, S., Tartari, G., 2014. Surrogate measures for providing high frequency estimates of total phosphorus concentrations in urban watersheds. Water Res. 64, 265–277. https://doi.org/10.1016/j.watres.2014.07.009.

Viviano, G., Valsecchi, S., Polesello, S., Capodaglio, A., Tartari, G., Salerno, F., 2017. Combined use of caffeine and turbidity to evaluate the impact of CSOs on river water quality. Water Air Soil Poll. 228, 330. https://doi.org/10.1007/s11270-017-3505-3.

Yang, S., Büttner, O., Kumar, R., Jäger, C., Jawitz, J.W., Rao, P.S.C., Borchardt, D., 2019. Spatial patterns of water quality impairments from point source nutrient loads in Germany's largest national River Basin (Weser River). Sci. Total Environ. 697, 134145 https://doi.org/10.1016/j.scitotenv.2019.134145.